# Quo Vadis NMR?

[Svatý Petr](#) je v době Neronova pronásledování křesťanů přesvědčen svými stoupenci, aby odešel z Říma do bezpečí. Cestou potkává [Ježíše Krista](#), který kráčí do města, a Petr se ho překvapeně ptá: *„Quo vadis, Domine?“* (Kam kráčíš, Pane?), *„Když ty opouštíš můj lid, jdu do Říma, aby mě ukřižovali podruhé.“*, odpovídá mu Ježíš. Poté se Petr obrací nazpět a později umírá na kříži stejně jako jeho Pán. Z pokory však, aby Ježíše nenapodoboval, si Sv. Petr vyprosí, aby jej ukřižovali jinak – hlavou dolů.
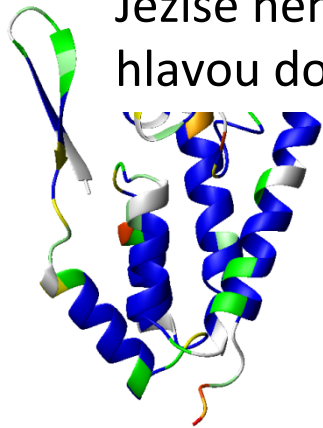
CANT

MUP-I

CSP-1

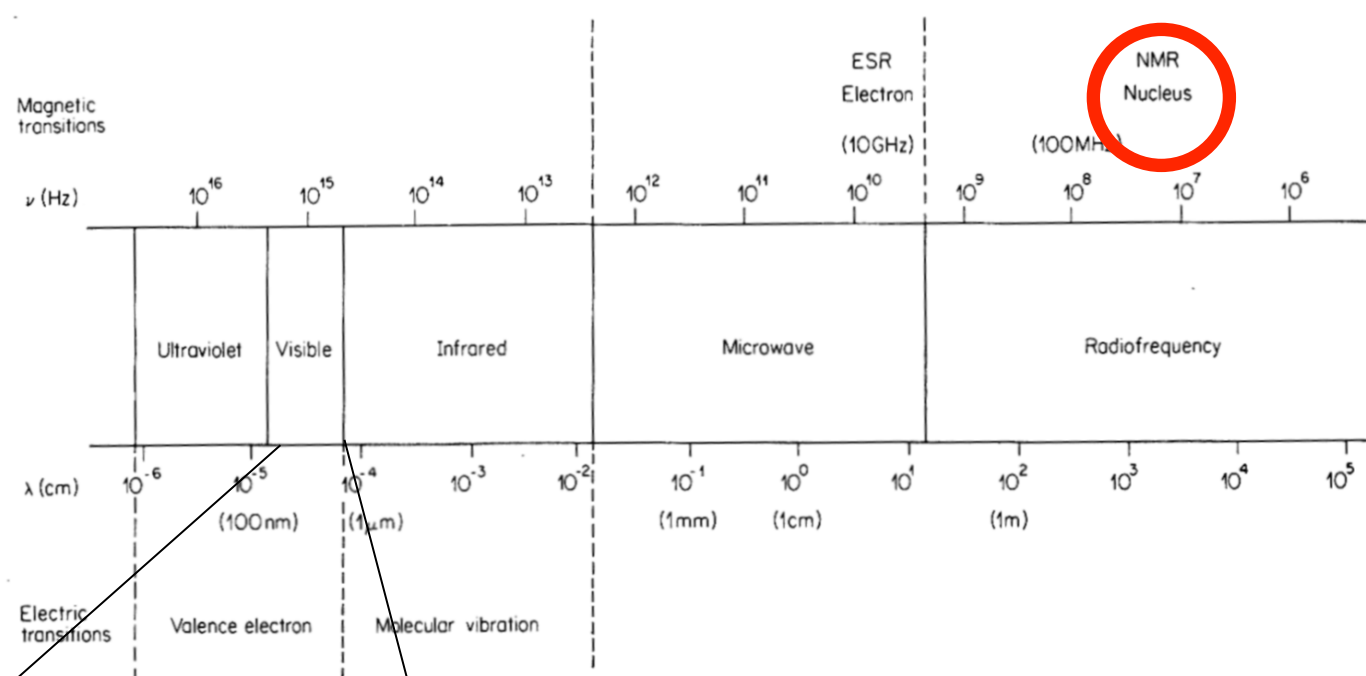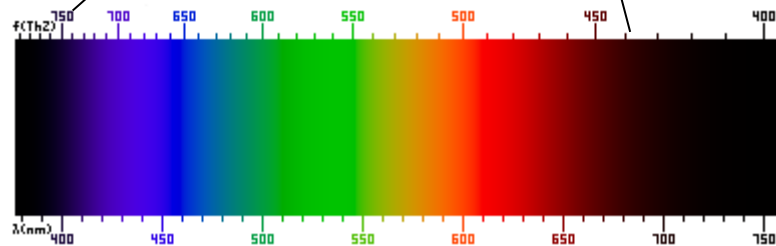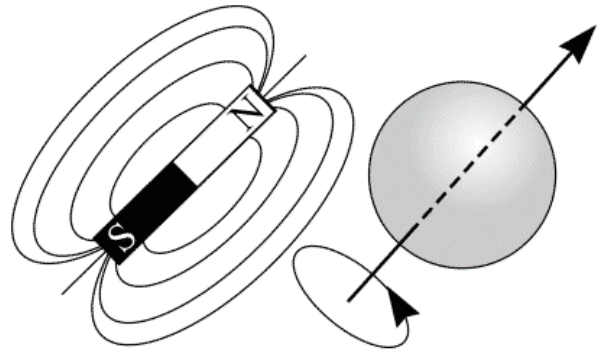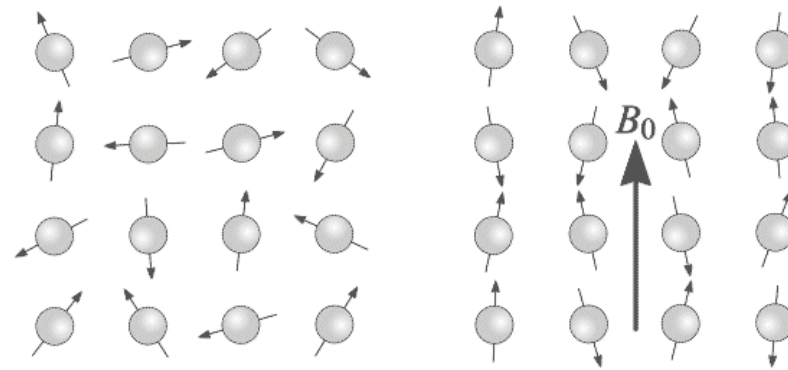merase

1
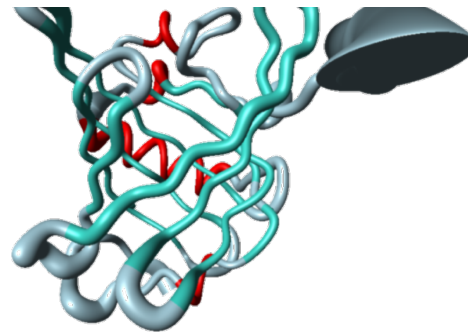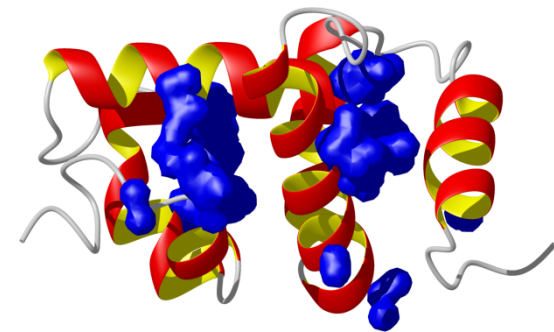
NMR

$$E = h.\nu$$

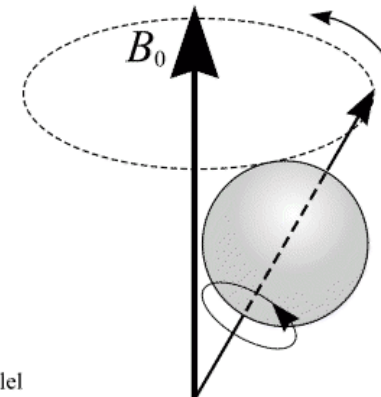Figure 1.2   Spectral regions of the electromagnetic spectrum of interest in biological investigations

1945 · · · · **1952**

$$\omega = \gamma \cdot B_o$$

E

B_0

θ

θ

Parallel

Anti-parallel

B_0

B_0
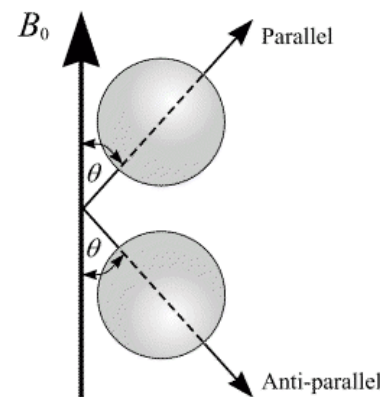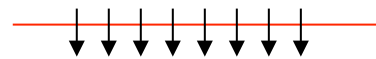
$$\nu = \gamma \cdot B_o / 2\pi \cdot (1 - \sigma) \sim 10 - 1000 \text{ MHz}$$
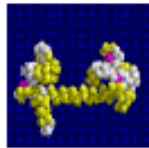
The NMR spectrum of ethanol

Methylene

$CH_3 — CH_2 — OH$

Methyl

Methyl triplet

Methylene quartet
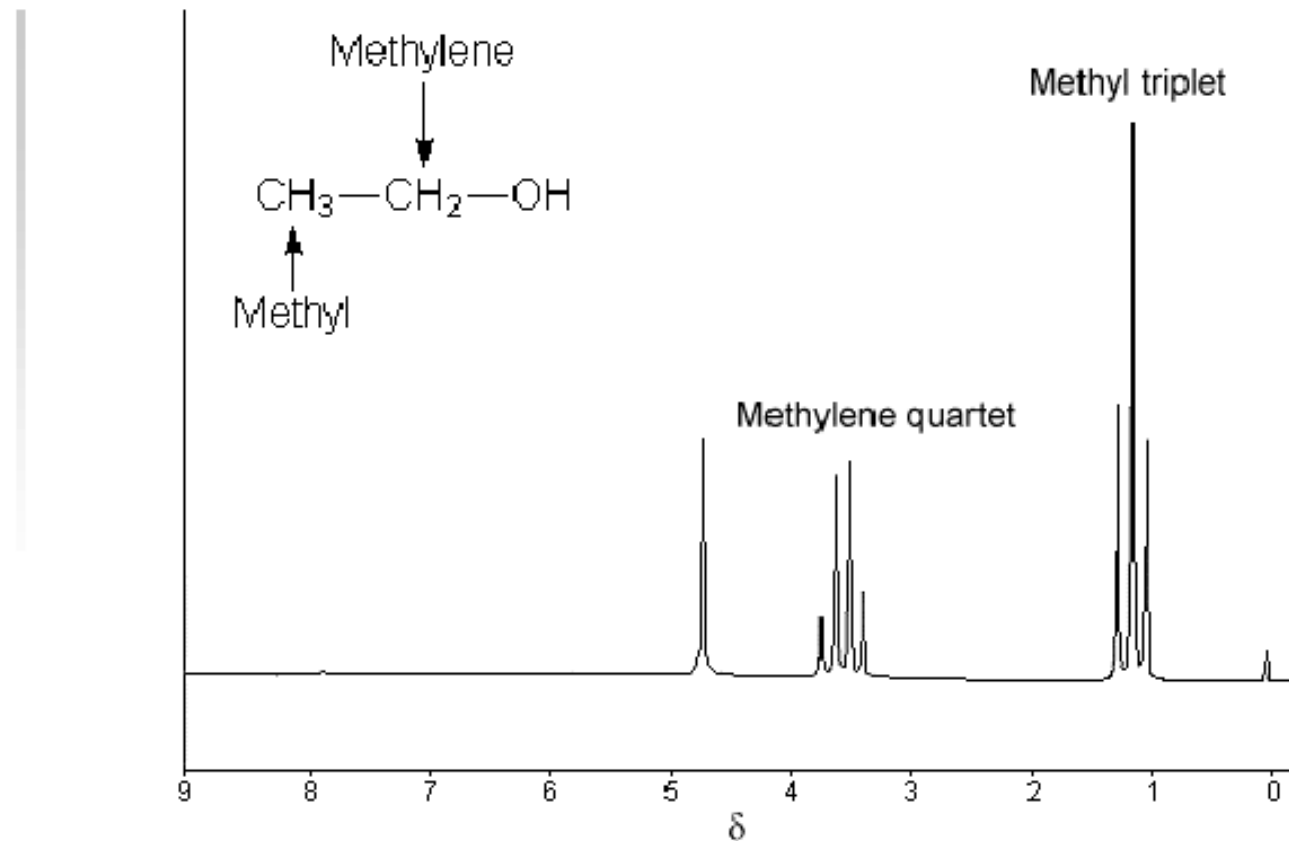
Classical Spectroscopy: dν/dt or dB/dt

$$\nu = \gamma.B_o./2\pi.(1 - \sigma)$$

x-y plane

Receiver Coil

M

Signal Amplitude

1.0

0.5

0.0

-0.5

-1.0

Time
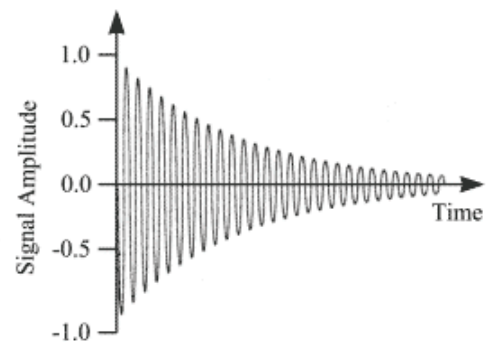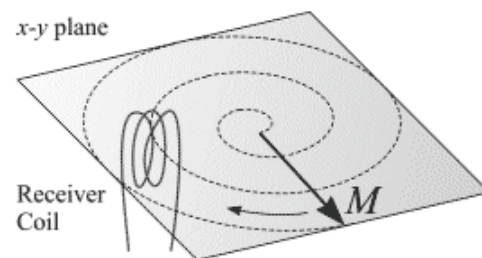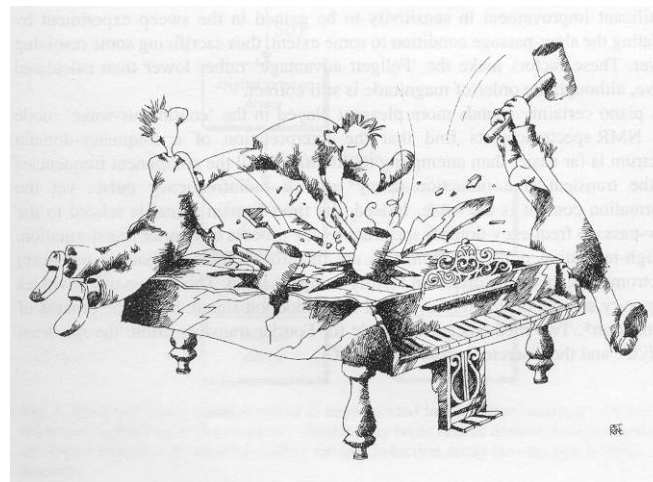
Fourier Transform

Joseph Fourier
(1768 – 1830)

Jean Baptiste Joseph Fourier
born Auxerre, March 21, 1768
died, Paris, May 16, 1830

He took a prominent part in his own district in promoting the revolution, and was rewarded by an appointment in 1795 in the Normal school, and subsequently by a chair in the Polytechnic school.

Fourier went with Napoleon on his Eastern expedition in 1798, and was made governor of Lower Egypt.

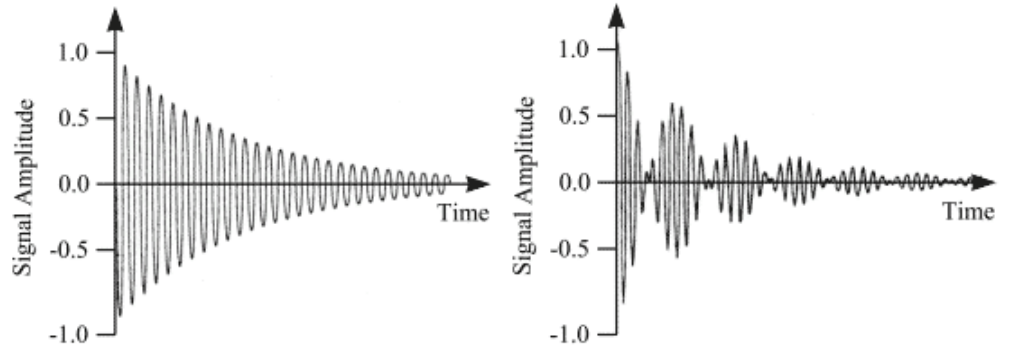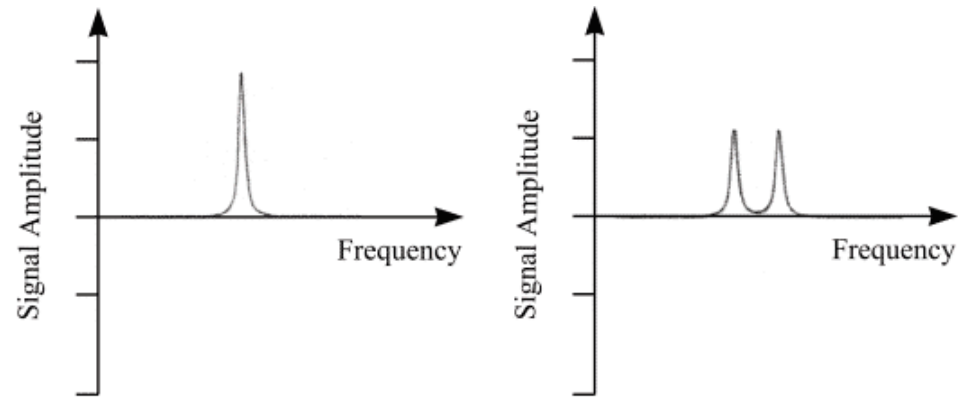**After the British victories and the capitulation of the French under General Menou in 1801, Fourier returned to France, and was made prefect of Grenoble, and it was while there that he made his experiments on the propagation of heat. He moved to Paris in 1816. In 1822 he published his *Théorie analytique de la chaleur*, in which he shows that any functions of a variable, whether continuous or discontinuous, can be expanded in a series of sines of multiples of the variable - a result which is constantly used in modern analysis.**

J.W.Cooley and J.W.Tukey, *Math. Comp*. 1965, 19, 297
Fast Fourier Transform

1D NMR

2D NMR

3D NMR

nD NMR

69

NMR

Felix Bloch
(1905-1983)

Edward M. Purcell
(1912-1997)

Resonance Absorption by Nuclear Magnetic Moments in a Solid

E. M. PURCELL, H. C. TORREY, AND R. V. POUND*
Radiation Laboratory, Massachusetts Institute of Technology,
Cambridge, Massachusetts,
December 24, 1945

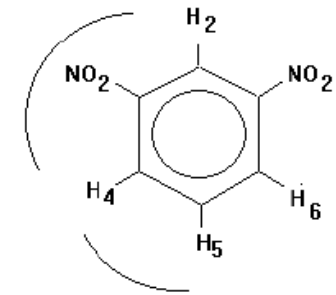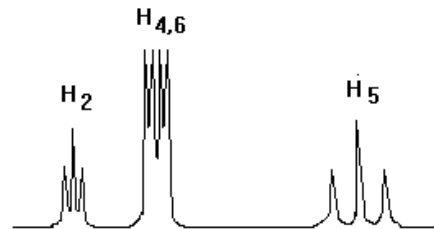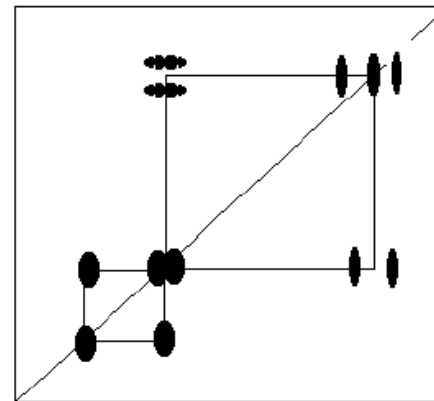IN the well-known magnetic resonance method for the determination of nuclear magnetic moments by molecular beams,[1] transitions are induced between energy levels which correspond to different orientations of the nuclear spin in a strong, constant, applied magnetic field. We have observed the absorption of radiofrequency energy, due to such transitions, in a *solid* material (paraffin) containing protons. In this case there are two levels, the separation of which corresponds to a frequency, ν, near 30 megacycles/sec., at the magnetic field strength, H, used in our experiment, according to the relation $h\nu = 2\mu H$. Although the difference in population of the two levels is very slight at room temperature ($h\nu/kT \sim 10^{-5}$) the number of nuclei taking part is so large that a measurable effect is to be expected providing thermal equilibrium can be established. If one assumes that only the real fields of importance are caused by the moments of neighboring nuclei, one can show that the imaginary part of the magnetic permeability, at resonance, would be of the order $h\nu/kT$. The absence of appreciable dispersion of the nuclear moment and the fact that the product of these factors upon absorption cross section per nucleus and density of nuclei is just cancelled by their influence on the width of the observed resonance.

A crucial question concerns the time required for the establishment of thermal equilibrium between spins and lattice. A difference in the populations of the two levels is a prerequisite for the observed absorption, because of the relation between absorption and stimulated emission. Moreover, unless the relaxation time is very short the absorption of energy from the radiofrequency field will equalize the population of the levels, more or less rapidly, depending on the strength of this r-f field. In the expectation of a long relaxation time (several hours), we chose to use so weak an oscillating field that the absorption would persist for hours regardless of the relaxation time, once thermal equilibrium had been established.

A resonant cavity was made in the form of a short section of coaxial line loaded heavily by the capacity of an end plate. It was adjusted to resonate at about 30 mc/sec. Input and output coupling loops were provided. The inductive part of the cavity was filled with 850 cm³ of paraffin, which remained at room temperature throughout the experiment. The resonator was placed in the gap of the large cosmic-ray magnet in the Research Laboratory of Physics, at Harvard. Radiofrequency power was introduced into the cavity at a level of about 10^{-11} watts. The radiofrequency magnetic field in the cavity was everywhere perpendicular to the steady field. The cavity output was balanced in phase and amplitude against another portion of the signal generator output. Any residual signal, after amplification and detection, was indicated by a microammeter.

With the r-f circuit balanced the strong magnetic field was slowly varied. An extremely sharp resonance absorption was observed. At the peak of the absorption the deflection of the output meter was roughly 20 times the magnitude of fluctuations due to noise, frequency, instability, etc. The absorption reduced the cavity output by 0.4 percent, and as the loaded Q of the cavity was 670, the imaginary part of the permeability of paraffin, at resonance, was about $3 \cdot 10^{-6}$, as predicted.

Resonance occurred at a field of 7100 oersteds, and a frequency of 29.8 mc/sec., according to our rather rough calibration. We did not attempt a precise calibration of the field and frequency, and the value of the proton magnetic moment inferred from the above numbers, 2.75 nuclear magnetons, agrees satisfactorily with the accepted value, 2.7896, established by the molecular beam method.

The full width of the resonance, at half value, is about 10 oersteds, which may be caused in part by inhomogeneities in the magnetic field which were known to be of this order. The width due to local fields from neighboring nuclei had been estimated at about 4 oersteds.

The relaxation time was apparently shorter than the time ($\sim$ one minute) required to bring the field up to the resonance value. The types of spin-lattice coupling suggested by I. Waller[2] fail by a factor of several hundred to account for a time so short.

The method can be refined in both sensitivity and precision. In particular, it appears feasible to increase the sensitivity by a factor of several hundred through a change in detection technique. The method seems applicable to the precise measurement of magnetic moments (strictly, gyromagnetic ratios) of most moderately abundant nuclei. It provides a way to investigate the interesting question of spin-lattice coupling. Incidentally, as the apparatus required is rather simple, the method should be useful for standardization of magnetic fields. An extension of the method in which the r-f field has a rotating component should make possible the determination of the sign of the moment.

The effect here described was sought previously by Gorter and Broer, whose experiments are described in a paper[3] which came to our attention during the course of this work. Actually, they looked for dispersion, rather than absorption, in LiCl and KF. Their negative result is perhaps to be attributed to one of the following circumstances: (a) the applied oscillating field may have been so strong, and the relaxation time so long, that thermal equilibrium was destroyed before the effect could be observed—(b) at the low temperatures required to make the change in permeability easily detectable by their procedure, the relaxation time may have been so long that thermal equilibrium was never established.
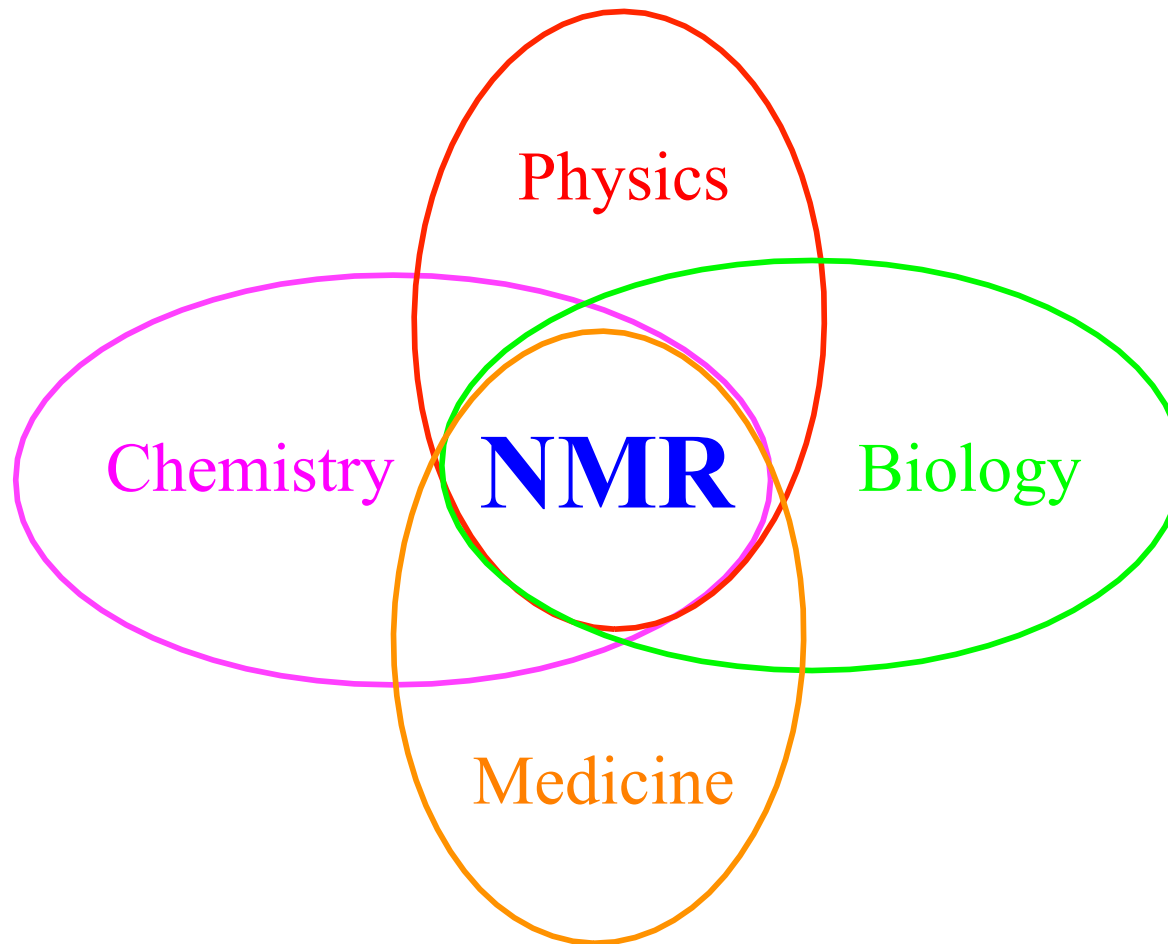
* Harvard University, Society of Fellows (on leave).
[1] Rabi, Zacharias, Millman, and Kusch, Phys. Rev. **53**, 318 (1938).
[2] I. Waller, Zeits. f. Physik **79**, 370 (1932).
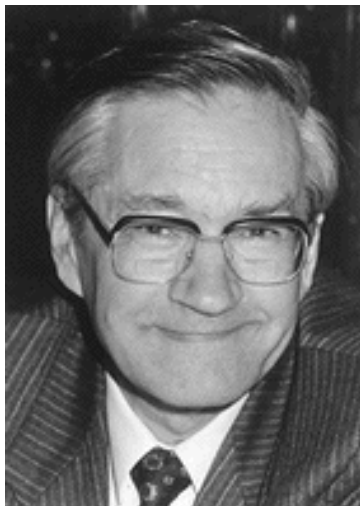[3] Gorter and Broer, Physica **9**, 591 (1942).

Figure 8 The first report of a nuclear magnetic resonance in a bulk material.[21] (Reproduced by permission of the American Physical Society)

For References see p. 143

9

Nuclear Induction

F. BLOCH, W. W. HANSEN, AND MARTIN PACKARD
Stanford University, Stanford University, California
January 29, 1946

THE nuclear magnetic moments of a substance in a constant magnetic field would be expected to give rise to a small paramagnetic polarization, provided thermal equilibrium be established, or at least approached. By superposing on the constant field (z direction) an oscillating magnetic field in the x direction, the polarization, originally parallel to the constant field, will be forced to precess about that field with a latitude which decreases as the frequency of the oscillating field approaches the Larmor frequency. For frequencies near this magnetic resonance frequency one can, therefore, expect an oscillating induced voltage in a pick-up coil with axis parallel to the y direction. Simple calculation shows that with reasonable apparatus dimensions the signal power from the pick-up coil will be substantially larger than the thermal noise power in a practicable frequency band.

We have established this new effect using water at room temperature and observing the signal induced in a coil by the rotation of the proton moments. In some of the experiments paramagnetic catalysts were used to accelerate the establishment of thermal equilibrium.

By use of conventional radio techniques the induced voltage was observed to produce the expected pattern on an oscillograph screen. Measurements at two frequencies showed the effect to occur at values H of the constant field that the ratio H/ν had the same value. Within our experimental error this ratio agreed with the value for protons, as determined by Kellogg, Rabi, Ramsey, and Zacharias.[1]

We have thought of various investigations in which this effect can be used fruitfully. A detailed account will be published in the near future.

[1] J. M. B. Kellogg, I. I. Rabi, N. F. Ramsey, and J. R. Zacharias, Phys. Rev. **56**, 738 (1939).

Figure 9 The first report of nuclear induction.[22] (Reproduced by permission of the American Physical Society)

Physical Review 69, 37 (1946)

Physical Review 69, 127 (1946)

Nuclear Magnetic Resonance
68 years
1945 – 2014

Nobel Prize in Chemistry 1991

Richard R. Ernst (1933 - *)
Swiss Federal Institute of Technology (ETH), Zürich, Switzerland

*"for his contributions to the development of the methodology
of high resolution nuclear magnetic resonance (NMR) spectroscopy"*

# Nobel Prize in Chemistry 2002

Kurt Wüthrich (1938 - *)
Swiss Federal Institute of Technology (ETH), Zürich, Switzerland
and The Scripps Research Institute, La Jolla, USA

*"for his development of nuclear magnetic resonance spectroscopy
for determining the three-dimensional structure of biological macromolecules in
solution".*

Nobel Prize in Physiology or Medicine 2003

Paul C. Lauterbur (1929 - 2007)
Biomedical Magnetic Resonance Laboratory, University of Illinois, Urbana, USA
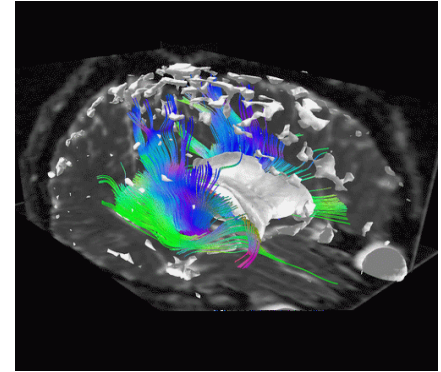
Sir Peter Mansfield (1933 - *)
Department of Physics, University of Nottingham, UK

for their discoveries concerning "magnetic resonance imaging"
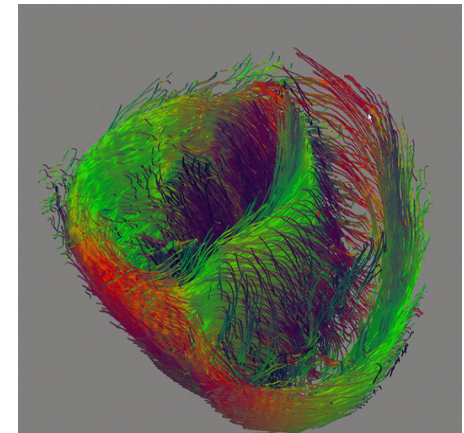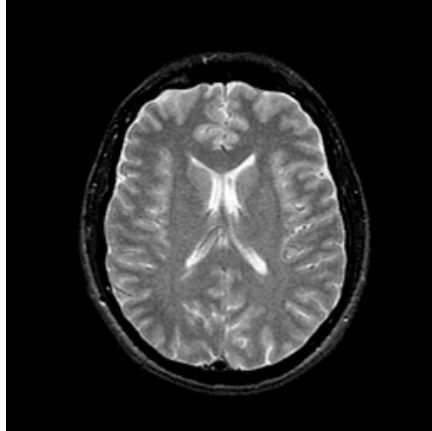
Human Brain
AIDS dementia
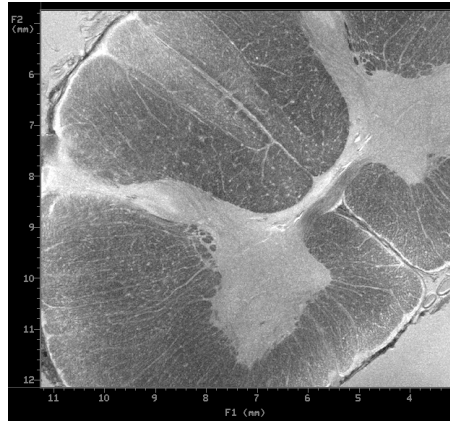
Spinal cord
μm resolution
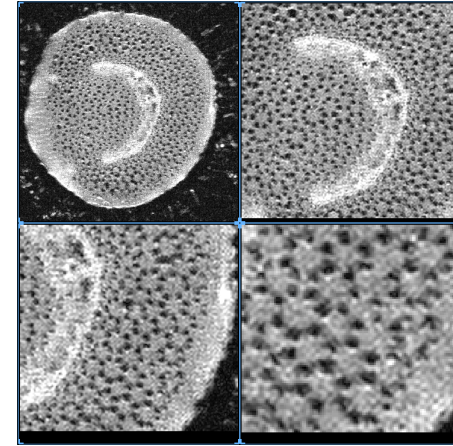
Plants

Birthday cake
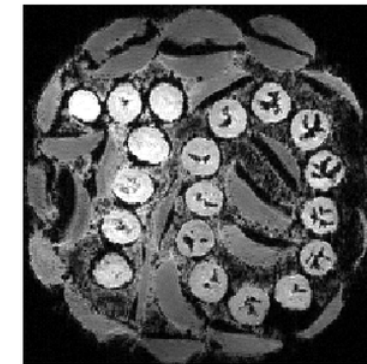
Milestones of NMR History

1945 Detection of NMR signals in bulk materials

1949 Discovery of chemical shift

1950 Discovery of spin-spin coupling

1952 Bloch and Purcell receive Nobel Prize

1953 First commercial NMR spectrometer (Varian 30MHz)

1966 Fourier transform (FT) techniques introduced – R.R. Ernst

1971 Two-dimensional (2D) NMR concept suggested – J. Jeener

1973 Zeugmatography: first two-dimensional NMR image - P. Lauterbur

1974 2D-NMR techniques developed – R.R. Ernst

1985 First 3D structures of proteins from NMR data – K. Wüthrich

1991 Ernst receives Nobel Prize

2002 Wüthrich receives Noble Prize

2003 Lauterbur and Mansfield receive Nobel Prize

2009 1 GHz spectrometer (Bruker)

Magnet history

1967
90 MHz

1970
270 MHz

1979
400 MHz

1983
500 MHz

1995
800 MHz

1998
700 MHz
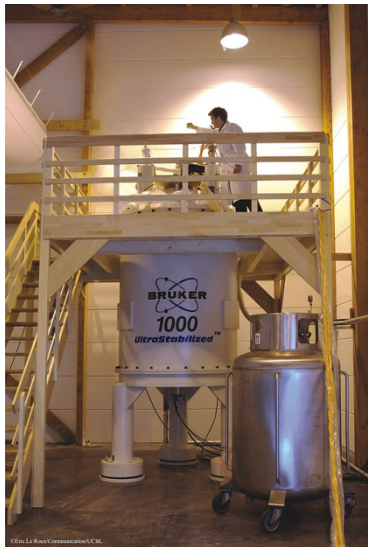
2009
1000 MHz

2005
950 MHz

2001
900 MHz

2000
800 US²

1999
750 WB

15

NMR as an eminent tool for structural and system biology
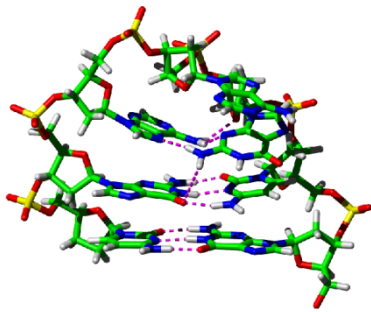
d(GCGAAGC)
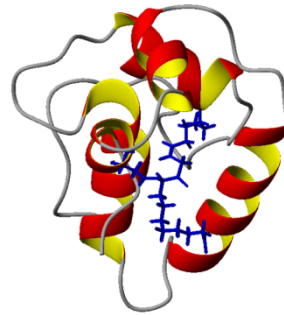
LTP-1
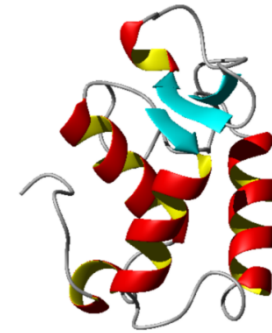
δ subunit of RNA polymerase
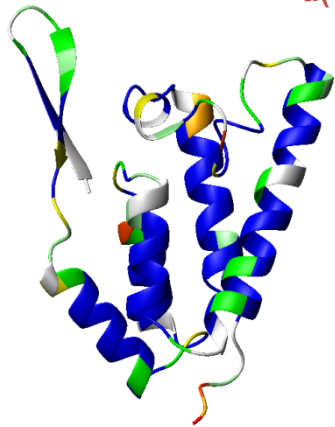
CANT
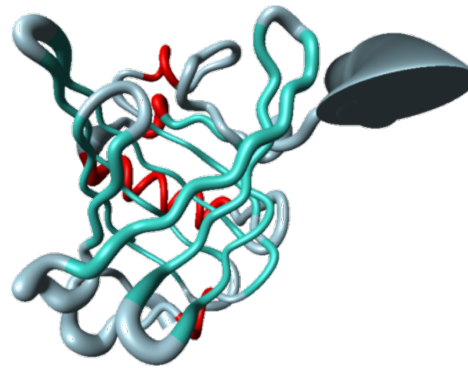
MUP-I
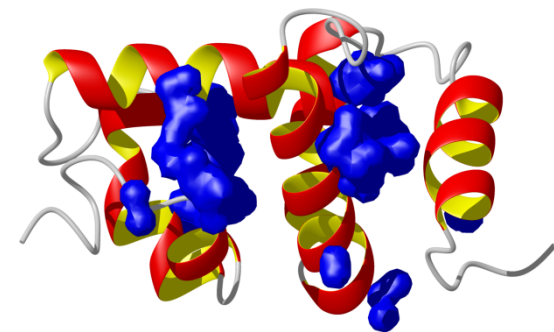
CSP-1

X-ray
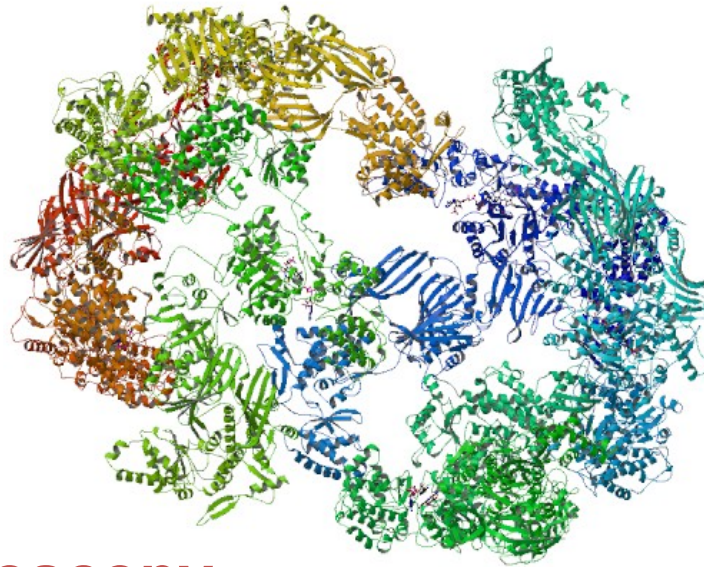
2.6-MD $\alpha6\beta6$ heterododecameric fatty acid synthase from Thermomyces lanuginosus at 3.1Å resolution

MS spectroscopy

EM microscopy
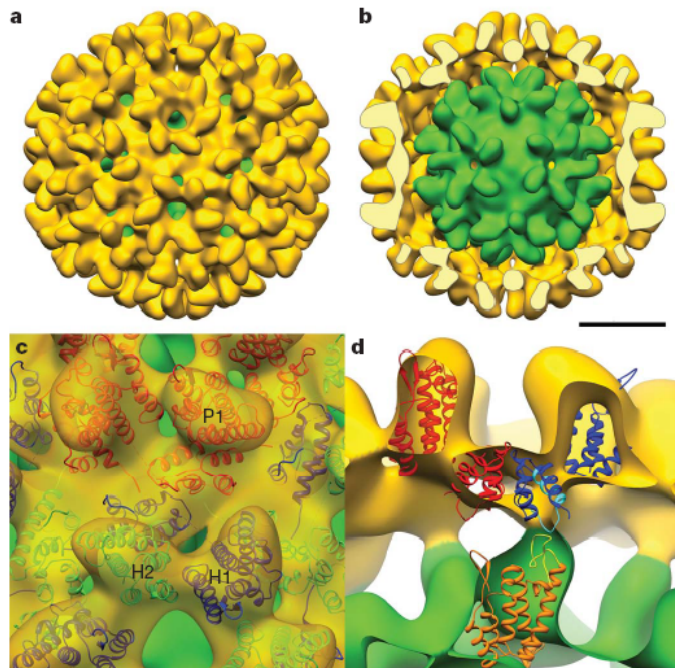
Features of Rous Sarcoma Virus capsid revealed by cryo electron microscopy and image reconstruction of the virion.

Monitoring the Assembly of the 20 S Proteasome
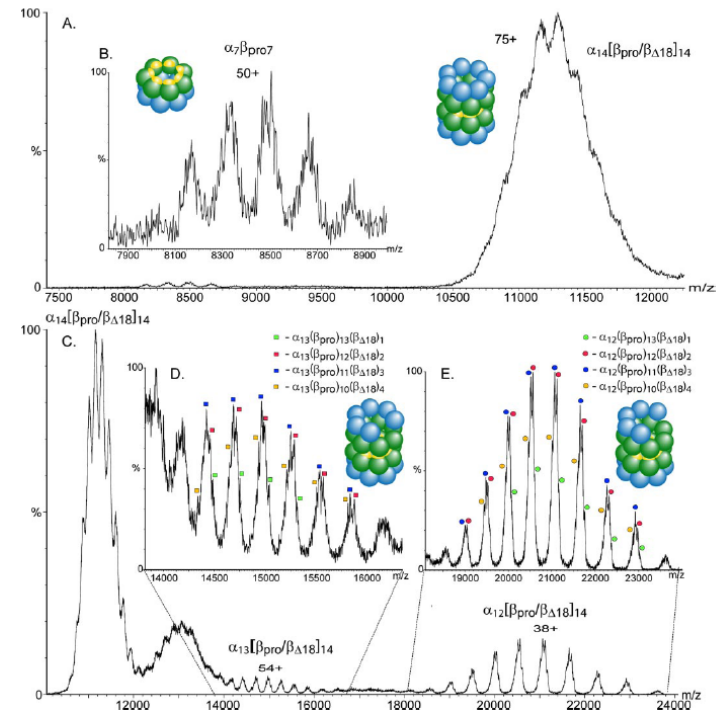
A real-time mass spectrometry approach to capture transient species along the assembly pathway of the 20 S proteasome

PDB Current Holdings Breakdown

	PROTEINS	NA	PROTEINS/NA complexes	OTHERS	TOTAL
X-ray	85540	1559	4551	5	91655
NMR	9291	1093	220	7	10611
ELECTRON MICROSCOPY	580	67	190	0	837
HYBRID	63	3	2	1	69
other	159	4	6	13	182
Total	95633	2726	4969	26	103354
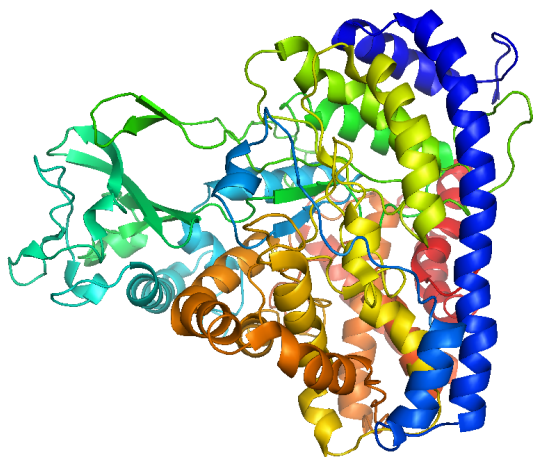
Solution global fold of the monomeric 723-residue (82-kDa) enzyme malate synthase G from *Escherichia coli* (Tugarinov V, Choy WY, Orekhov VY, Kay LE., *Proc Natl. Acad. Sci U.S.A.,* 18, 102:622-7, 2005).

723 aa Human genome

# of proteins

# of amino acids

18
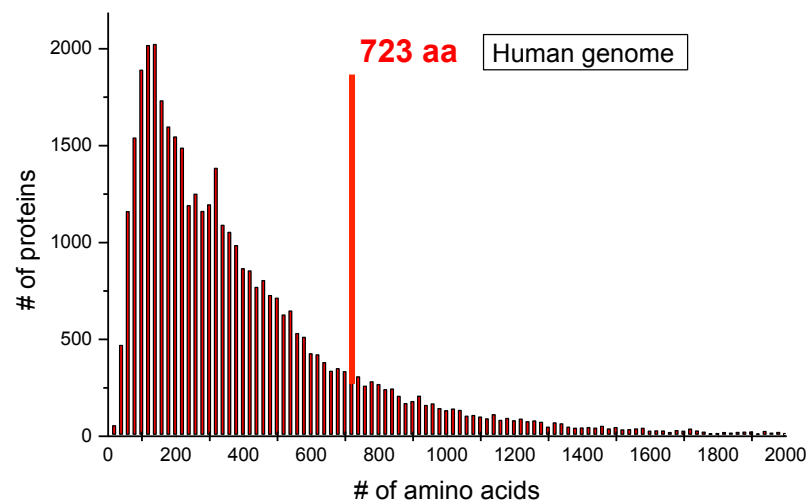
NMR
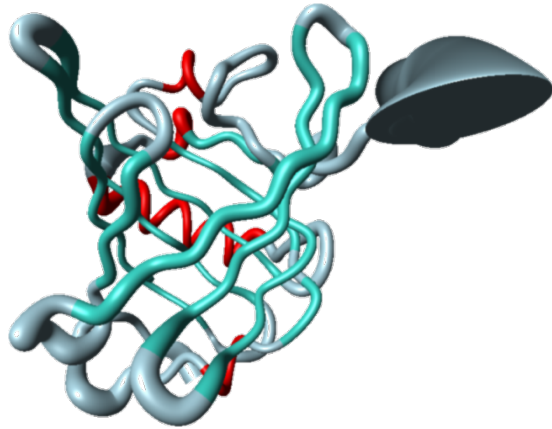
MD simulation
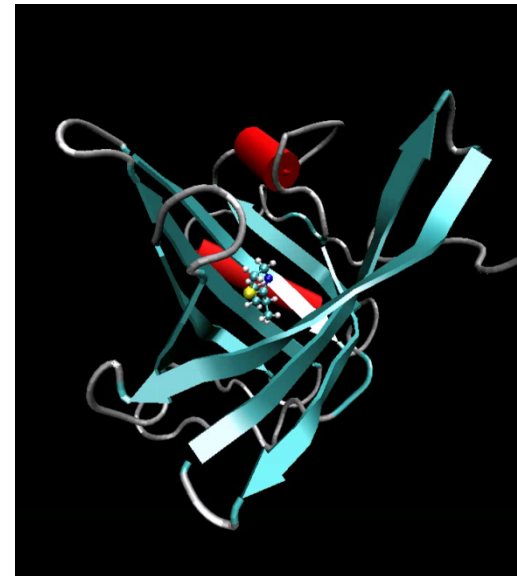
Time scales of high−resolution NMR

frequency   1GHz   1MHz   1000Hz   1Hz

time   1ps   1ns   1μs   1ms   1s

molecular tumbling

diffusion

internal motion

chemical reactions / exchange

chemical shifts

J−coupl.

relaxation: τ_c, internal motions

T_1, T_2, NOE
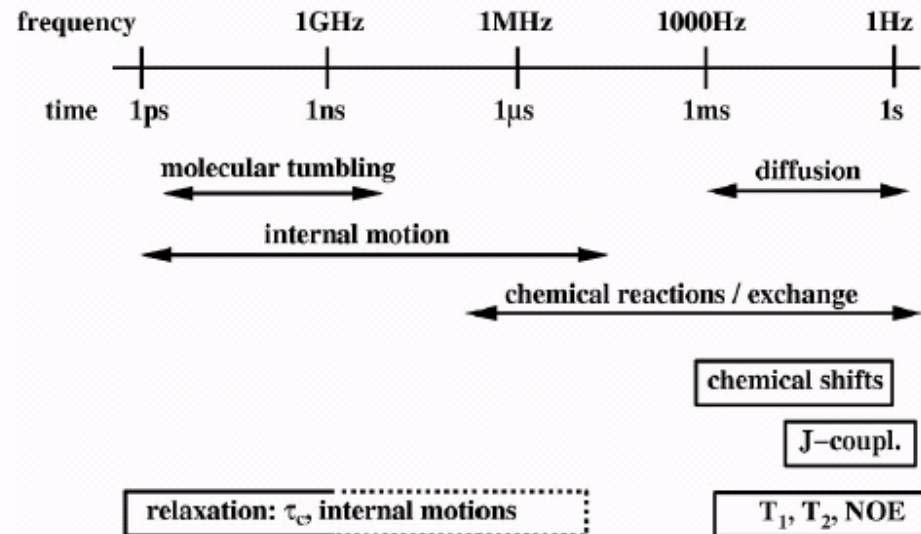
NMR of Biomacromolecules

1985 – 6.2 kDa
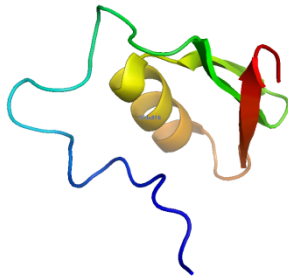
2005 – 82 kDa

Williamson, M.P. Havel, T.F. Wuthrich, K.
Solution conformation of proteinase inhibitor IIA from bull seminal plasma
by 1H nuclear magnetic resonance and distance geometry. *J.Mol.Biol. 182. 295-315 ,1985*
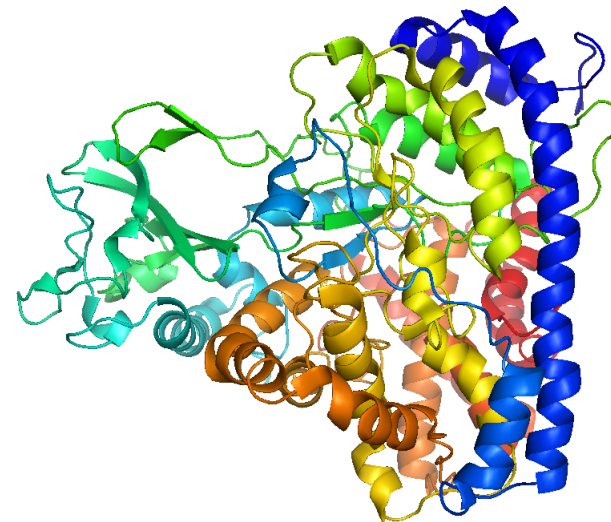
Vitali Tugarinov, Wing-Yiu Choy, Vladislav Yu. Orekhov, and Lewis E. Kay
Solution NMR-derived global fold of a monomeric 82-kDa enzyme, PNAS 2005 102: 622-627; published online before print January 6 2005, 10.1073/pnas.0407792102

Natural Abundance of NMR isotopes

| ^{1}H | 99.98 % | active in NMR |

^{12}C   98.9 %   non-active in NMR

| ^{13}C | 1.1 % | active in NMR |
| ^{15}N | 0.3 % | active in NMR |

| ^{31}P 100.0 % | active in NMR |

Isotope labeling by molecular biology methods

Isotope labeling of RNA

In vitro transcription with T7 RNA polymerase using isotopicaly labeled 5'-triphosphates (NTPs) as substrates

Production of $^{13}C,^{15}N$-labeled RNA

E. coli fermementation with N-15 amonium sulfate and/or C-13 glucose

↓

Isolation of rRNA

↓

Nuclease P-1 degradation of rRNA to rNMPs

↓

Enzymatic or chemical phosphorylation to rNTPs

↓

ATP   GTP   UTP   CTP

↓

RNA oligomer synthesis on a DNA template using T7 RNA polymerase

Basic principles of 3D structure determination by NMR

How Do We Go From Spectra to A Structure?

2D HSQC spectra

N-terminal domain of M-PMV
capsid protein

Resonance Assignments
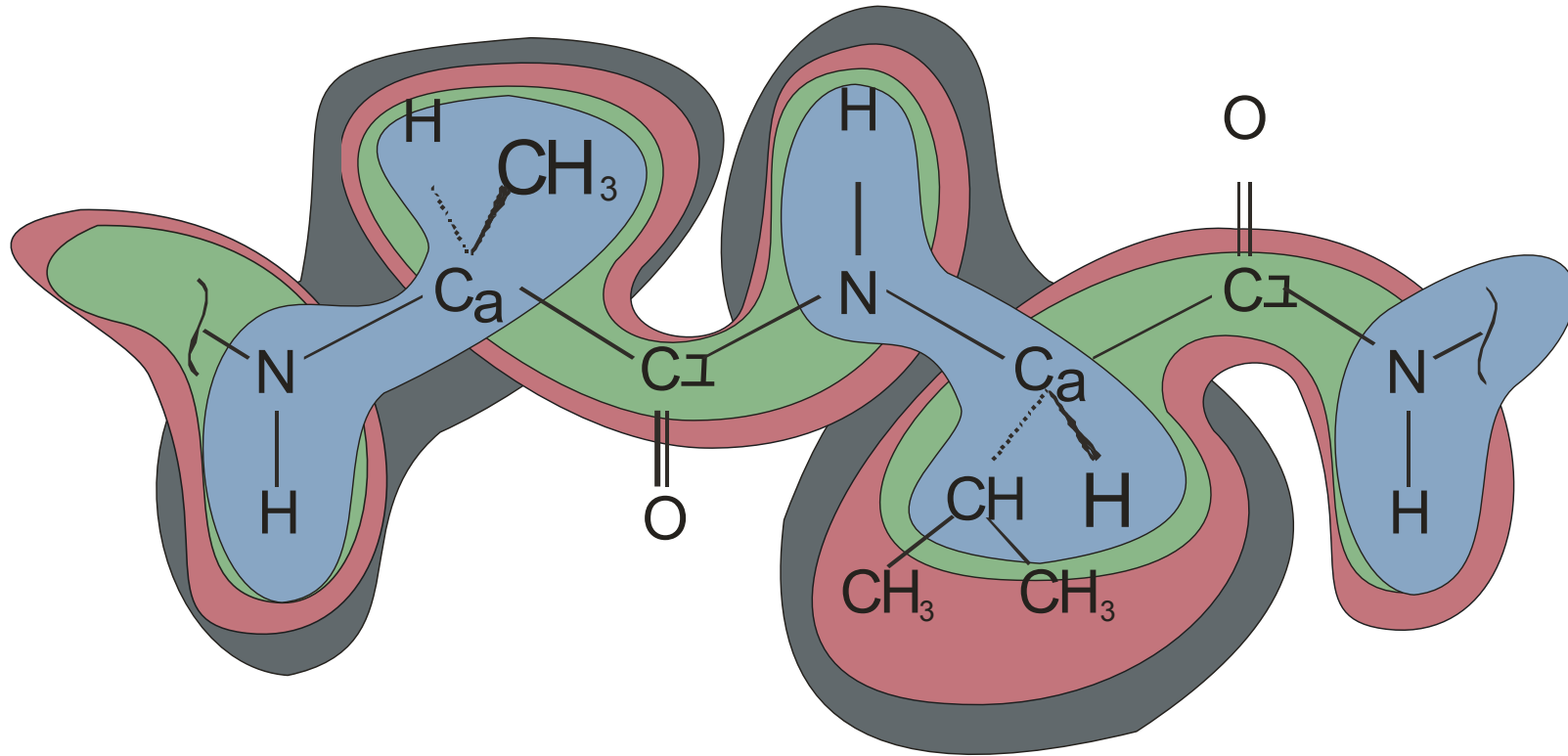
2D HSQC

3D CBCA(CO)NH

3D CBCANH

3D HCC(CO)NH-TOCSY

3D TOCSY-HSQC

Basic principles of 3D structure determination by NMR

NOE
- a through space correlation (<5Å)
- distance constraint

NOE

4.1Å

2.9Å
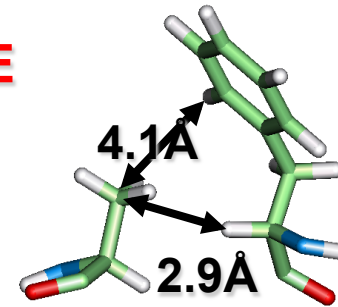
Coupling Constant (J)
- through bond correlation
- dihedral angle constraint

J

NH   CαH

CαH   NH
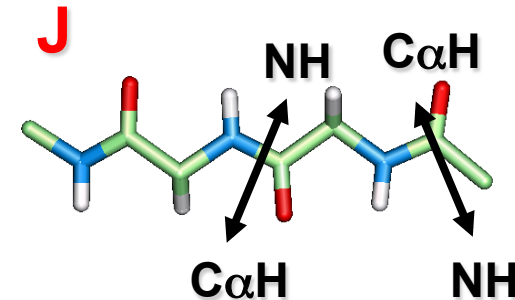
Chemical Shift
- very sensitive to local changes in environment
- dihedral angle constraint

Dipolar coupling constants (D)
- bond vector orientation relative to magnetic field
- alignment with bicelles or viruses

D
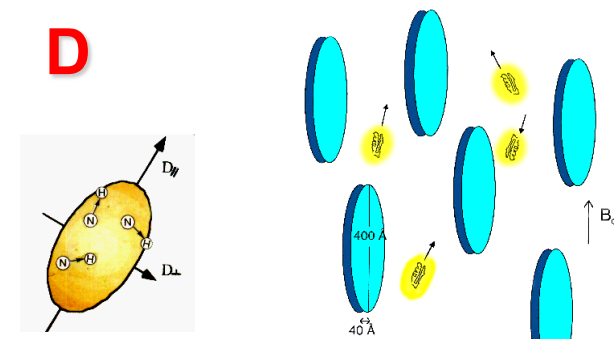
Dipolar couplings and induced changes of chemical shifts
(relative orientation of atom-atom vectors, dynamics)
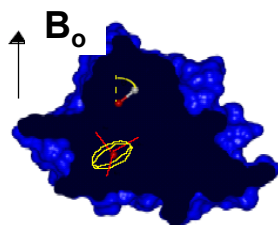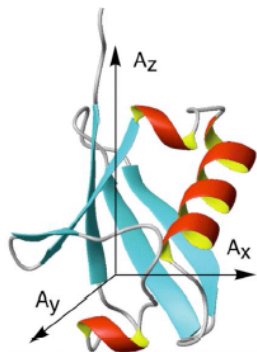
Non-averaging of DD interactions in aligned media
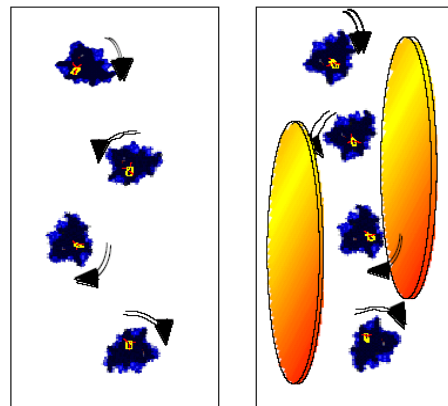
RDC - residual dipolar couplings

$$D^{AB}(\theta,\phi) = D_a(3\cos^2\theta - 1) + 3/2\ D_r(\sin^2\theta\ \cos^2\phi)]$$
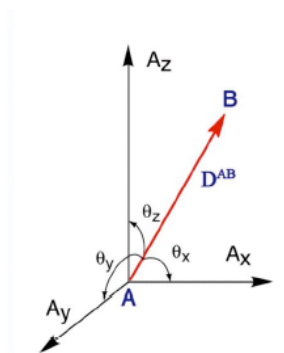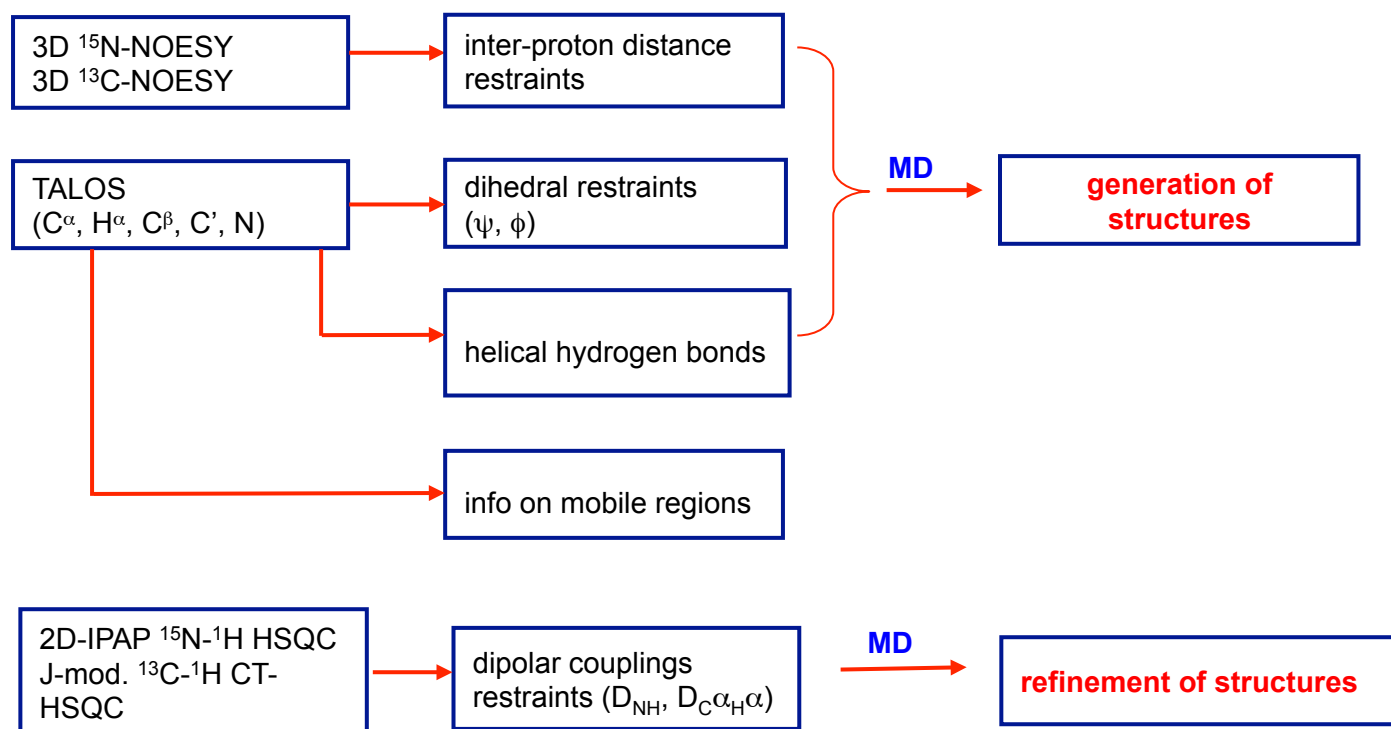
CSI - induced changes of isotropic chemical shifts
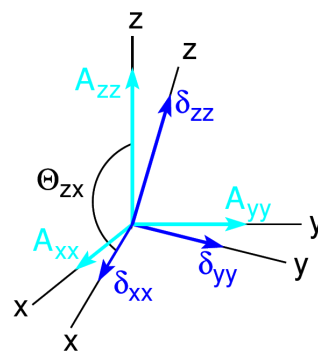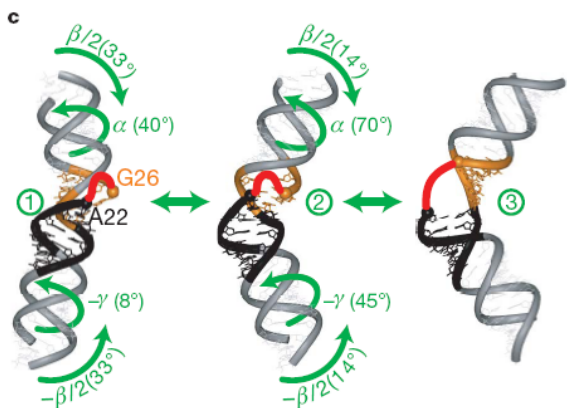
$$\Delta\delta_| = \frac{1}{3}\sum_{i=x,y,z}\sum_{j=x,y,z}A_{ii}\cos^2\theta_{ij}\delta_{jj}$$

Example of NMR structure determination

```
┌─────────────────────┐        ┌─────────────────────┐
│ 3D ¹⁵N-NOESY         │───────▶│ inter-proton distance│
│ 3D ¹³C-NOESY         │        │ restraints           │
└─────────────────────┘        └─────────────────────┘
```

3D ^{15}N-NOESY
3D ^{13}C-NOESY → inter-proton distance restraints

TALOS
(C^α, H^α, C^β, C', N) → dihedral restraints (ψ, ϕ)

→ helical hydrogen bonds

MD → **generation of structures**

TALOS → info on mobile regions

2D-IPAP ^{15}N-^{1}H HSQC
J-mod. ^{13}C-^{1}H CT-HSQC → dipolar couplings restraints (D_{NH}, $D_{C\alpha H\alpha}$)

MD → **refinement of structures**

Potential Energy Terms

$$E_{TOTAL} = E_{chem} + w_{exp}E_{exp}$$

$$E_{exp} = E_{NOE} + E_{torsion} + E_{H\text{-}bond} + E_{gyr} + E_{rama} + E_{RDC} + E_{CSA} + E_{para}$$

$$E_{chem} = E_{bond} + E_{angle} + E_{dihedral} + E_{vdw} + E_{electr}$$
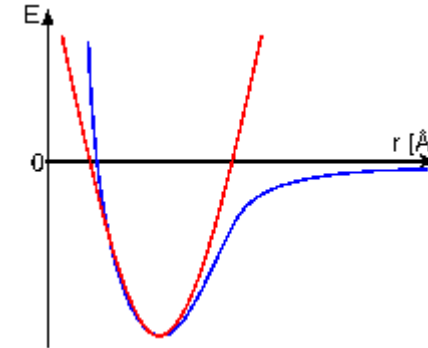
- E_{chem} : (*a priori* knowledge) primary structure, topology, covalent bonds, dihedral angles (harmonic), etc.
  - non-covalent van-der-Waals forces: Lennard-Jones potential
  - electrostatic interactions - Coulomb potential etc.

- E_{exp} : experimental constraint terms

Recent potential energy terms used in MD:

- dipolar couplings (E_{rdc})
- radius of gyration (E_{gyr})
- CSA (E_{CSA})
- side chain conformational database torsion angle potentials (E_{rama})
- paramagnetic relaxation enhancement module (E_{para})

Mason-Pfizer Monkey Virus
M-PMV

❑ 1970: Chopra, H.C., Mason, M.M. (mammary carcinoma of a female rhesus monkey - Macaca mulatta)

❑ Retroviridae, Oncovirinae, Betaretrovirus

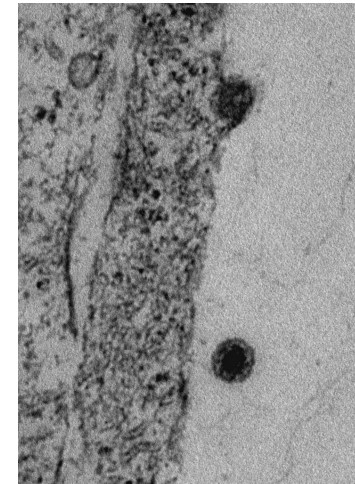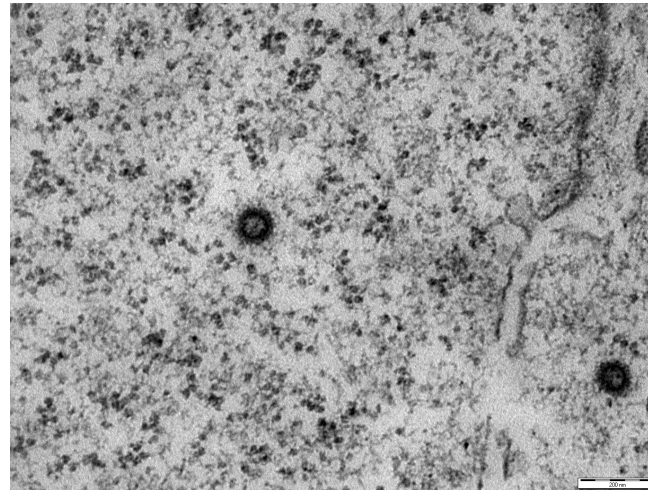❑ D type / C type (HIV)
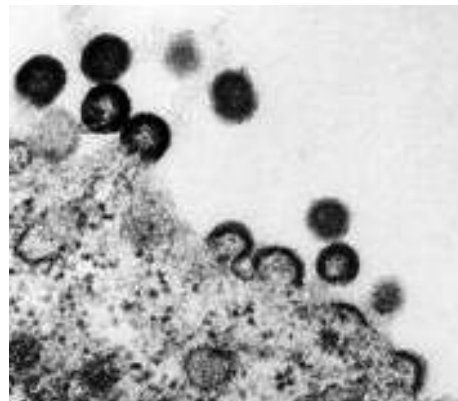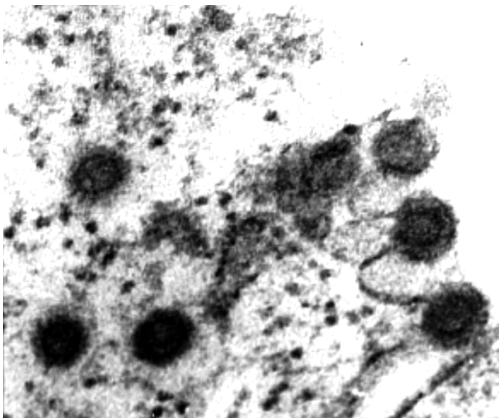
Assembly of immature viral particles

C-type HIV-1
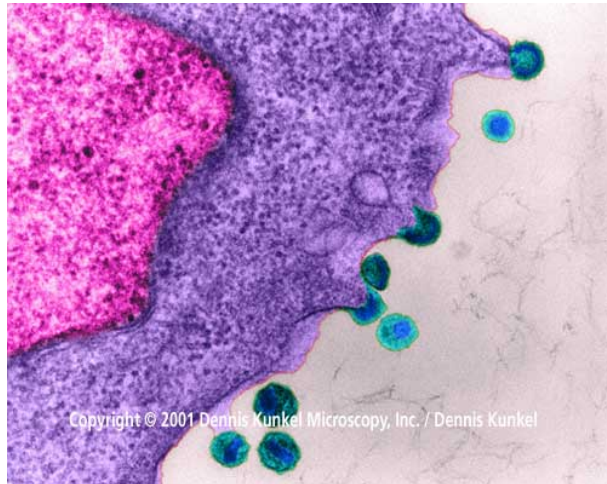
**D-type** M-PMV
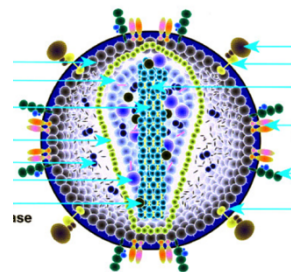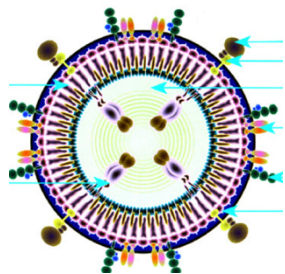
N-terminal domain of M-PMV capsid protein
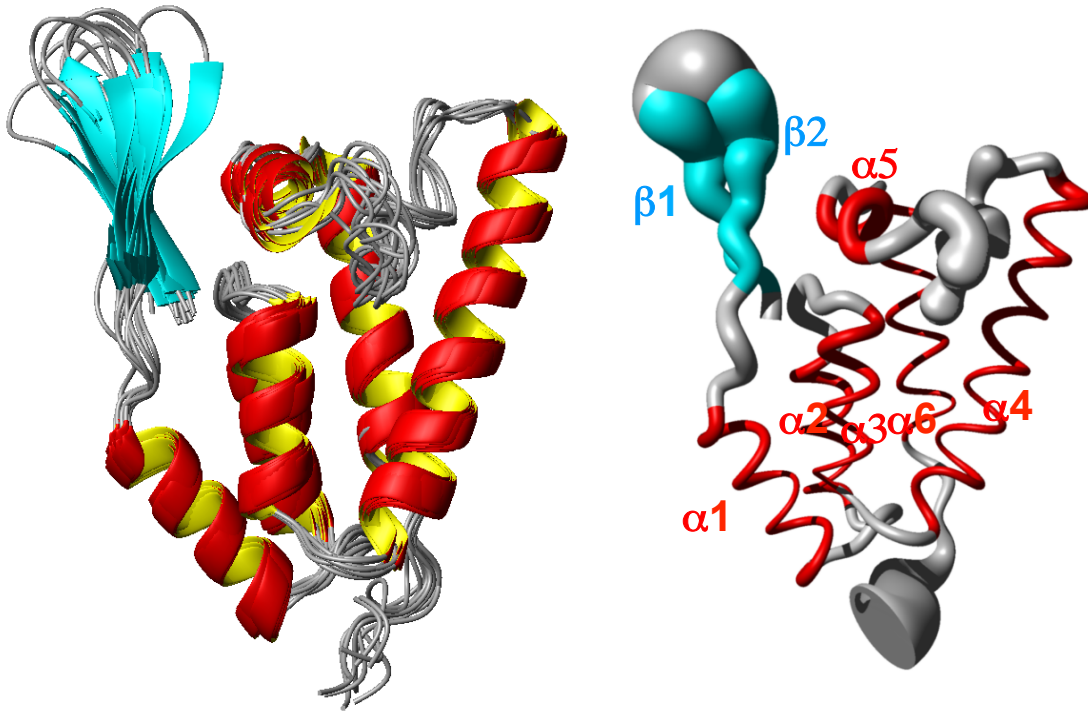
| Restraint Information	
Distance restraints	2246
Hydrogen bonding restraints	124
Torsion Angle restraints (φ/ψ)	107/107
Residual Dipolar Couplings	130
Average rms deviation from experimental restraints	
Distance restraints (Å)	0.023 ± 0.001
dihedral angle restraints (°)	0.552 ± 0.067
residual dipolar couplings (Hz)	1.811 ± 0.061
RDCs Q factor	0.225 ± 0.008
Violations	
distance violations > 0.5Å	0
dihedral angle violations > 5°	0
Pairwise Cartesian RMS deviation (Å)	
ordered all heavy atoms	1.60 ± 0.23
ordered backbone heavy atoms	1.11 ± 0.23
ordered all heavy atoms	1.24 ± 0.10	helices only
ordered backbone heavy atoms	0.74 ± 0.11	helices only

M-PMV
PDB 2KGF

MLV (X-ray)
PDB 3BP9
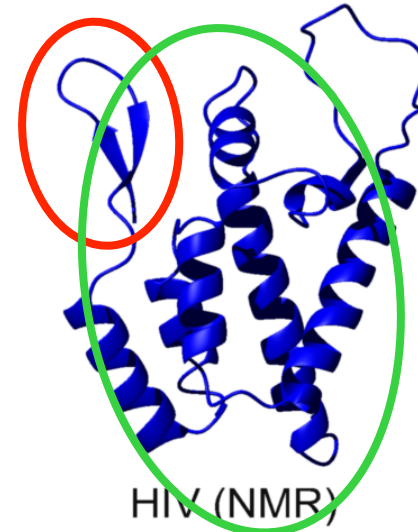
HIV (NMR)
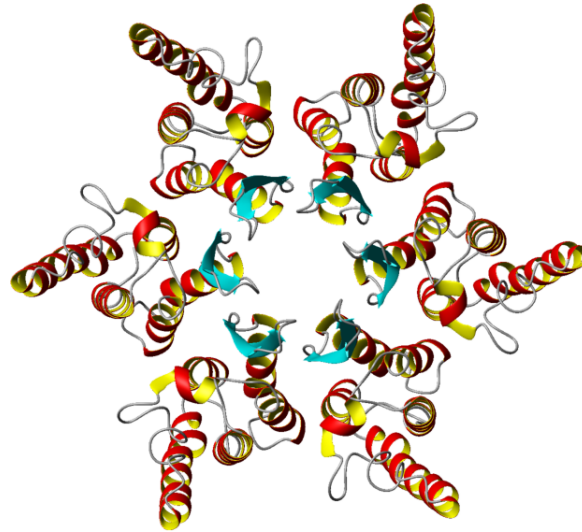PDB 1GWP
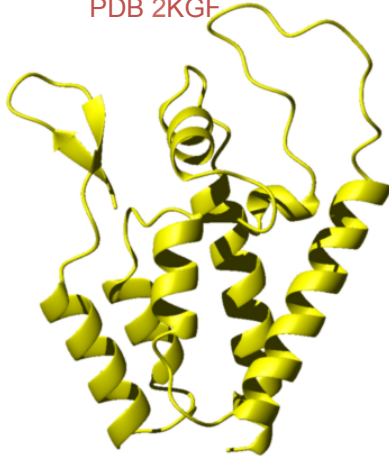
HIV (X-ray)
PDB 1AK4
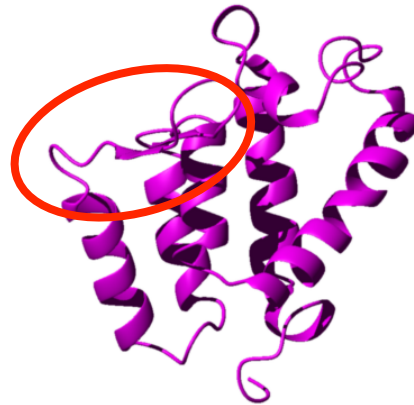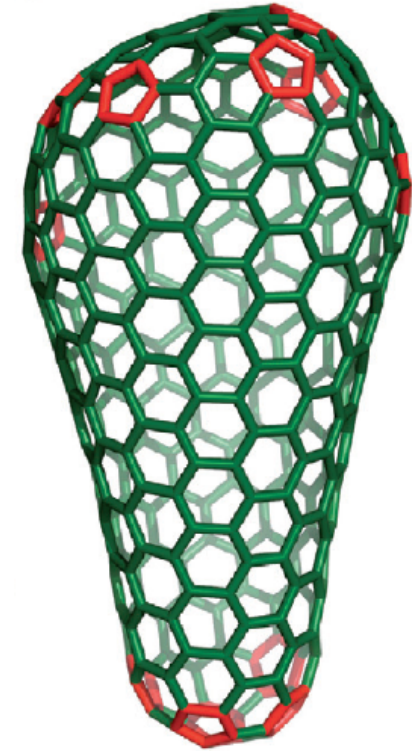
HTLV (NMR)
PDB 1G03

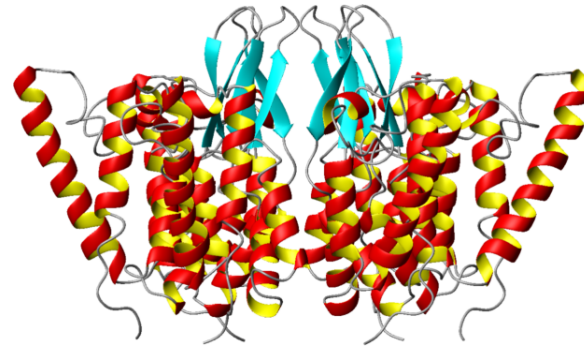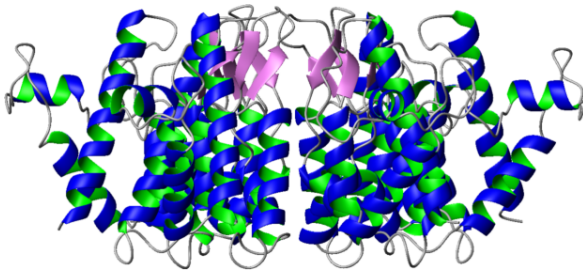RSV (X-ray)
PDB 1EM9

Pro-1

Asp-57
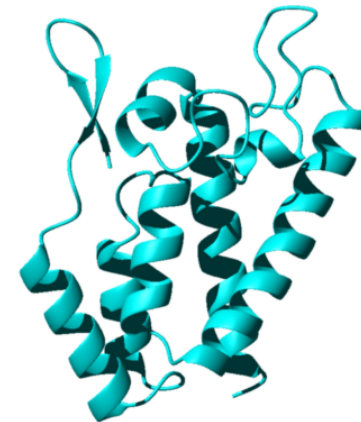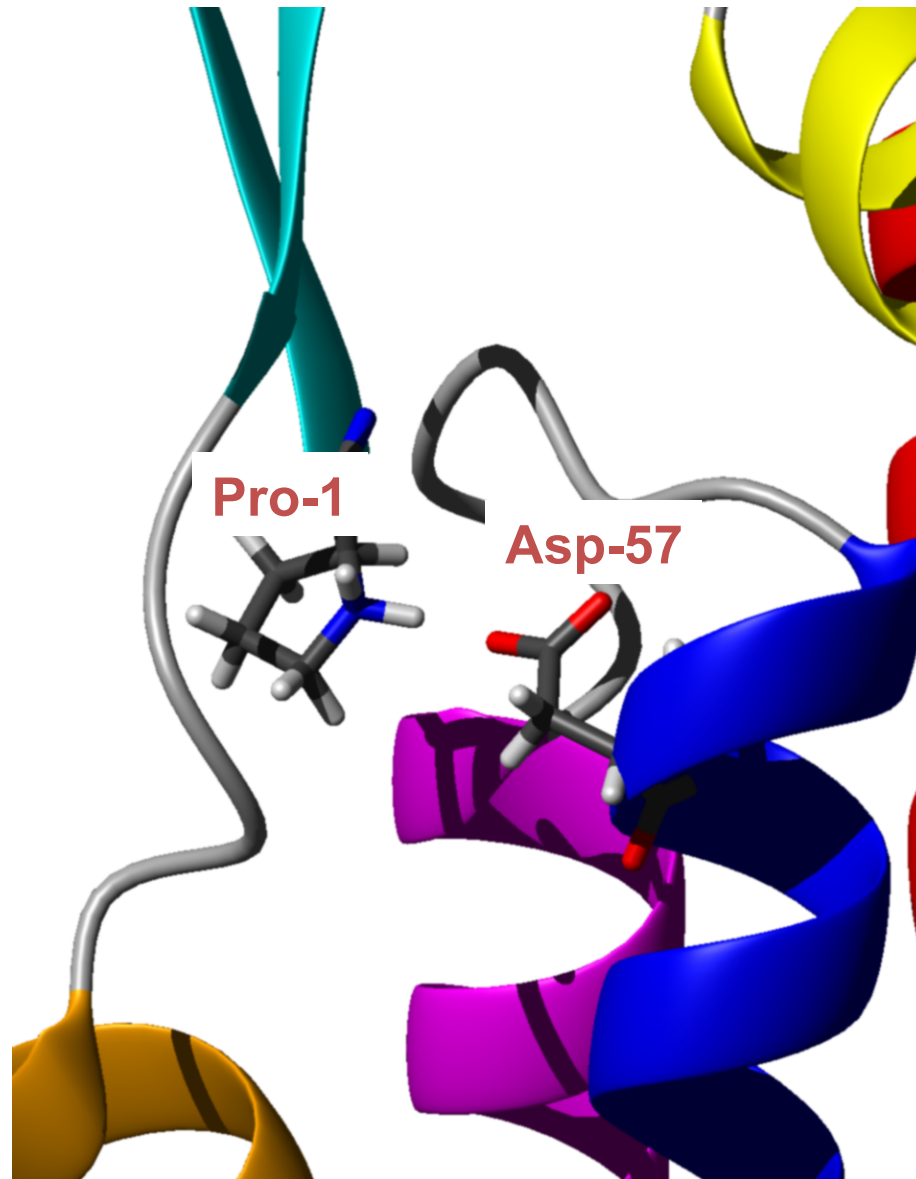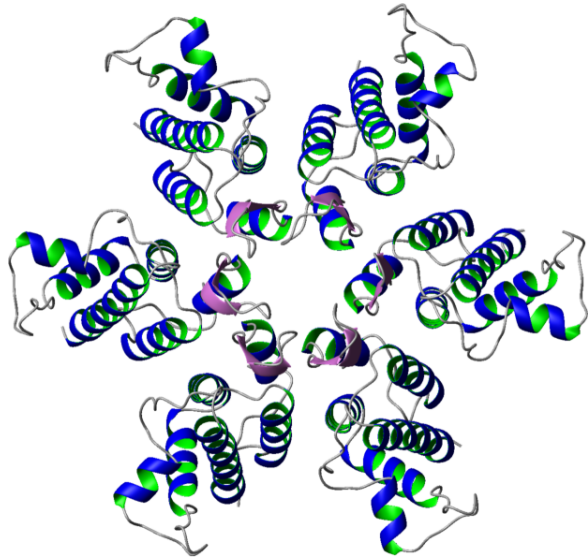
MLV CA-NT hexamer by x-ray
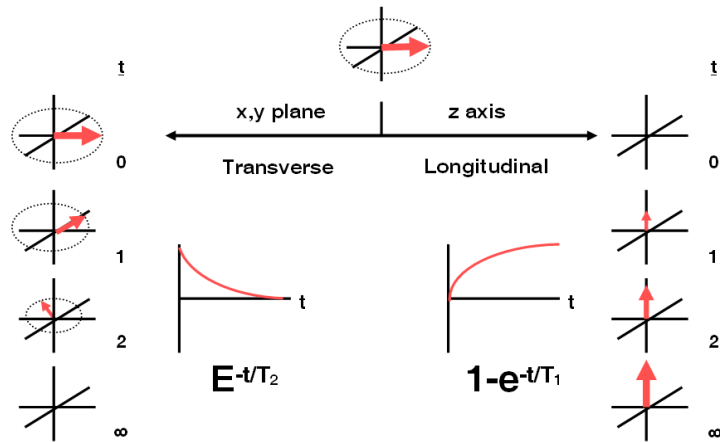(Mortuza, G.B. et al. JMB 376, 1493-1508, 2008)

M-PMV CA-NT hexamer
model from nmr data

Fullerene model for the conical
capsid, with CA hexamers
(Ganser-Pornillos, B.K. et al. COSB, 18,
203-217, 2008)

35

Dynamics and molecular motions

Heteronuclear relaxation ^{15}N, ^{13}C

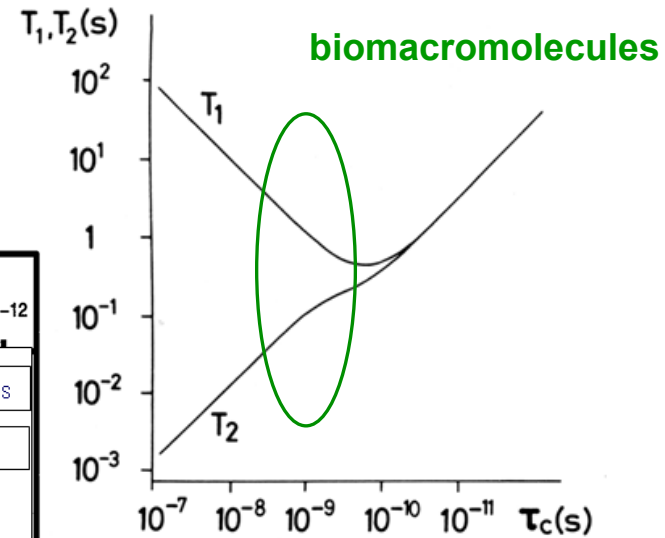T_1 – spin-lattice relaxation time– fast motions
T_2 – spin-spin relaxation time – fast & slow motions
^1H-^{15}N NOE – fast and some slow motions

biomacromolecules
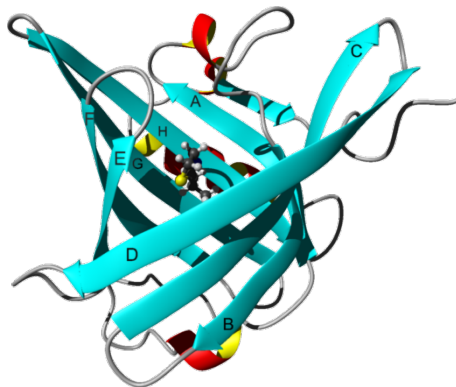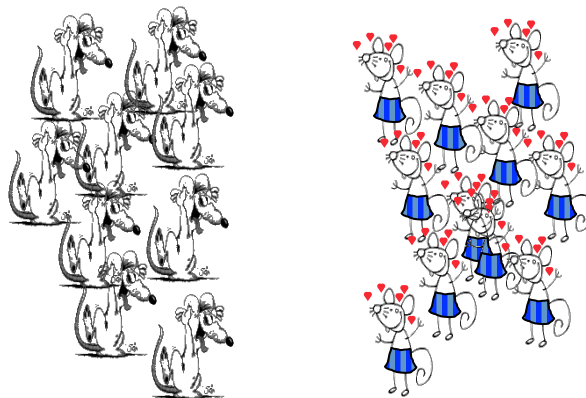
large ---- small
molecules

Quo vadis?
Molecular motions on ps -ns time scale

MUP – mouse urinary protein

Pheromones

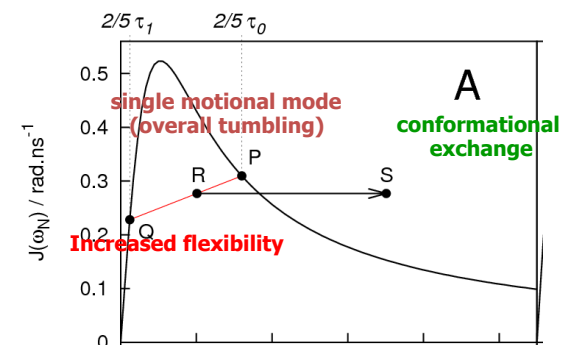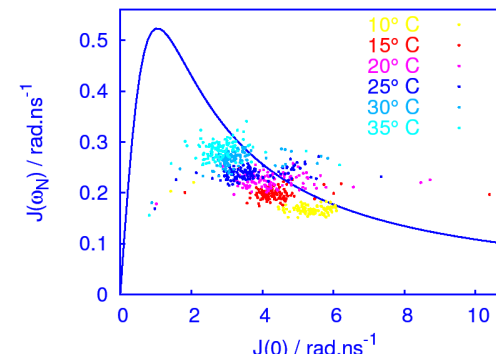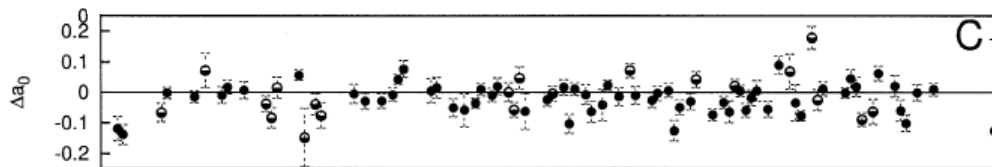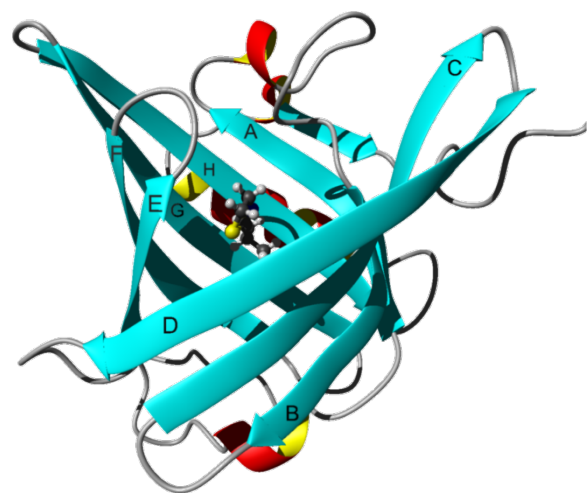$$\begin{pmatrix} J(0) \\ J(\omega_N) \\ J(0.87\omega_H) \end{pmatrix} = \begin{pmatrix} \frac{-3}{4(3d^2+c^2)} & \frac{3}{2(3d^2+c^2)} & \frac{-9}{10(3d^2+c^2)} \\ \frac{1}{(3d^2+c^2)} & 0 & \frac{-7}{5(3d^2+c^2)} \\ 0 & 0 & \frac{1}{5d^2} \end{pmatrix} \begin{pmatrix} \frac{1}{T_1} \\ \frac{1}{T_2} \\ \frac{\gamma_N}{\gamma_H}\frac{NOE-1}{T_1} \end{pmatrix}$$

Top right plot: $J(\omega_N)$ / rad.ns^{-1} vs $J(0)$ / rad.ns^{-1}; temperature legend 10° C, 15° C, 20° C, 25° C, 30° C, 35° C.

Middle right plot (A): $2/5\,\tau_1$, $2/5\,\tau_0$; **single motional mode (overall tumbling)**; **conformational exchange**; **Increased flexibility**; points Q, R, P, S.

Bottom right plot: Bound, Free; G 111; points f, b.

Bottom left plot (C): Δa_0.
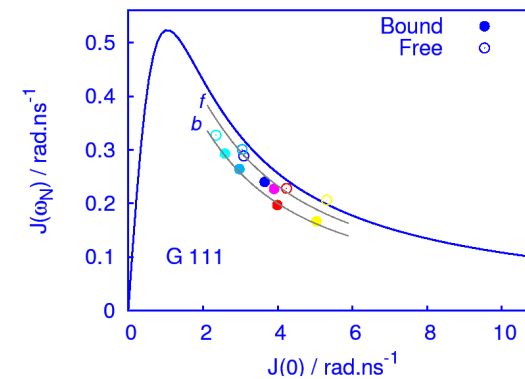
X-ray

Side chains
N35 and R60

MUP (120F) – PDB: 1YP7

10 MUP complexes

PDBs: 1QY0,1QY1, 1QY2, 1YP6, 1ZND, 1ZNE, 1ZNG, 1ZNH, 1ZNK, 1ZNL)

C D

L3

5 ns

12 ns

16 ns
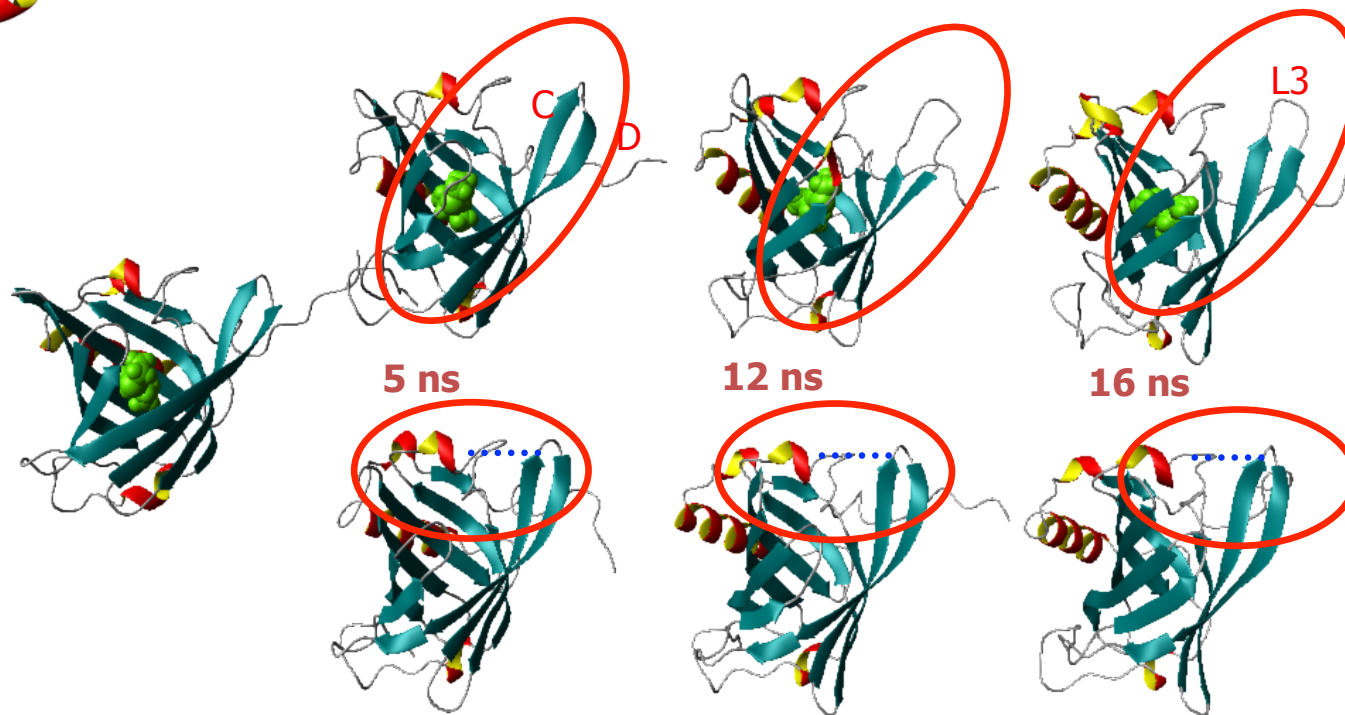
Start X-ray

Macek, P., Novák, P., Křížová, H., Žídek, L., and Sklenář, V.: *FEBS Letters*, **2006**, 580, 682-684: Molecular Dynamics Study of Major Urinary Protein – Pheromone Interactions: A Structural Model for Ligand-Induced Flexibility Increase.

Macek, P., Novák, P., Žídek, L., and Sklenář, V.: *J. Phys. Chem. B* **2007**, 111, 5731-5739:
Backbone Motions of Free and Pheromone-Bound Major Urinary Protein Studied by Molecular Dynamics Simulation.

Quo vadis?
Molecular complexes of increasing size and complexity

structure of SAM^{Vts1p} with RNA: a shape specific recognition

Oberstraaa et al. Nat. Struct. Biol. 13, 160-167, 2006
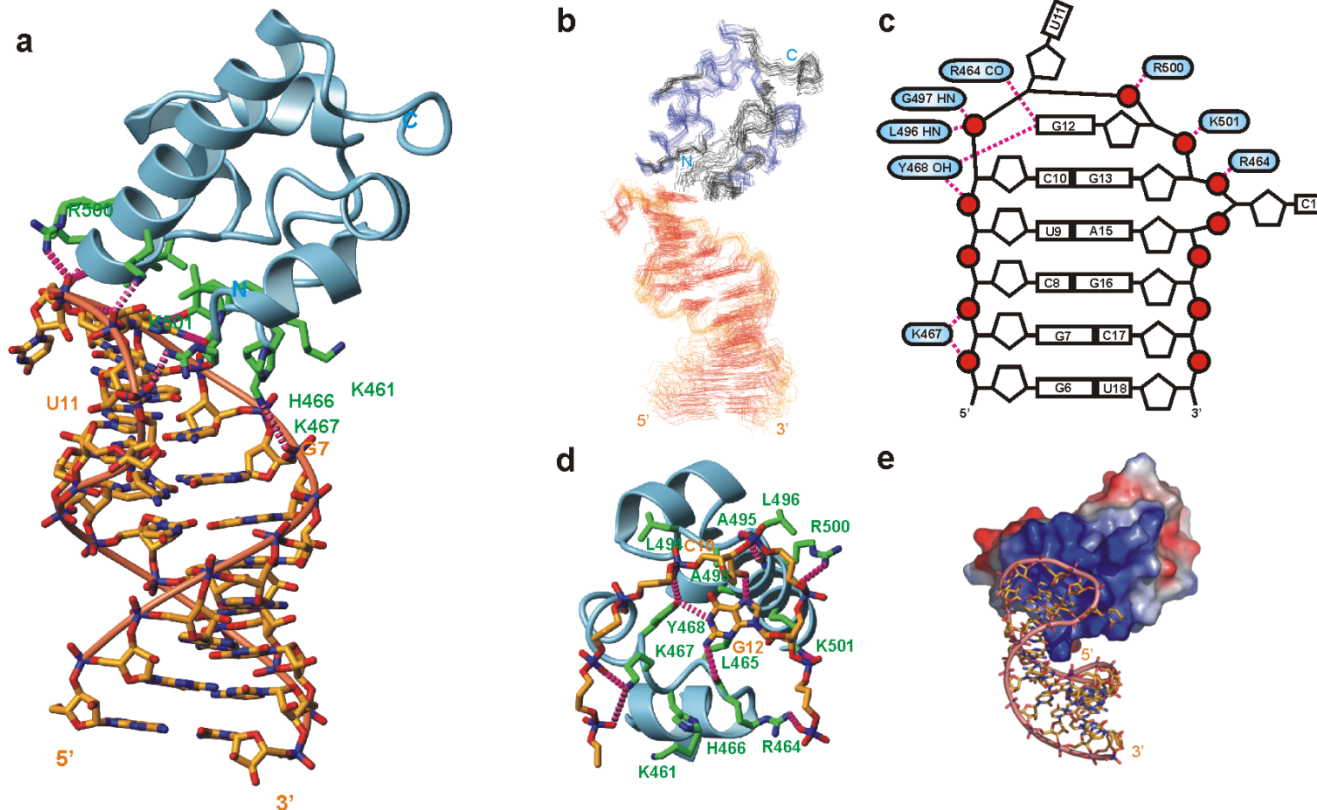
Quo vadis?
3D protein structure generation from NMR chemical shift data

CHESHIRE (CHEmical SHIft REstraints)

Michele Vendruscolo, Oxford

11 proteins in the size range of 46–123 residues, yielded results remarkably close (**1.3–1.8 Å backbone atom rmsd**; 2.1–2.6 Å rmsd for all atoms) to structures previously determined using conventional x-ray crystallography or NMR methods.

CS-ROSETTA

Ad Bax, Bethesda

16 proteins with known structures;
9 proteins with unknown structures for which only chemical shift assignments but no structural coordinates were available. **56 to 129 residues** full-atom models that have **0.7–1.8 Å backboe atom rmsd** to the experimentally determined x-ray or NMR structures.
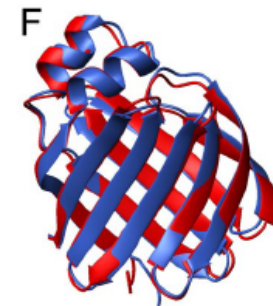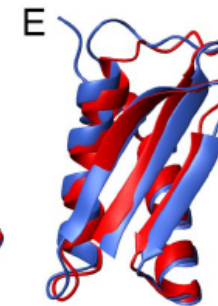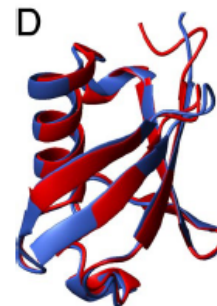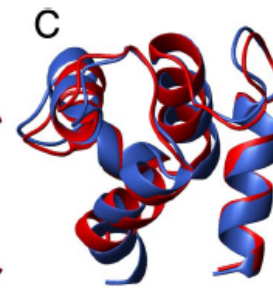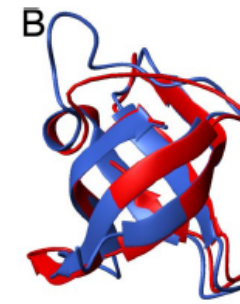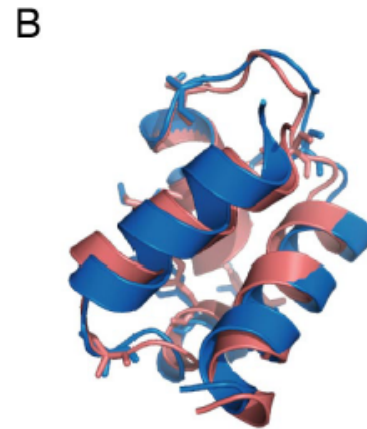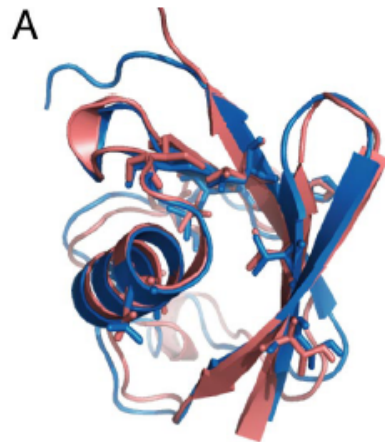
Quo vadis?
Characterization of weakly interacting molecular networks

INPHARMA method

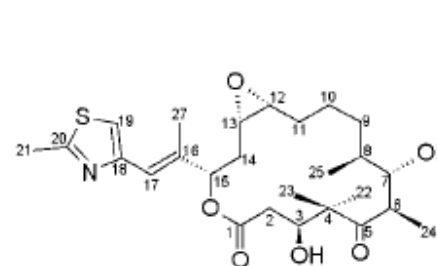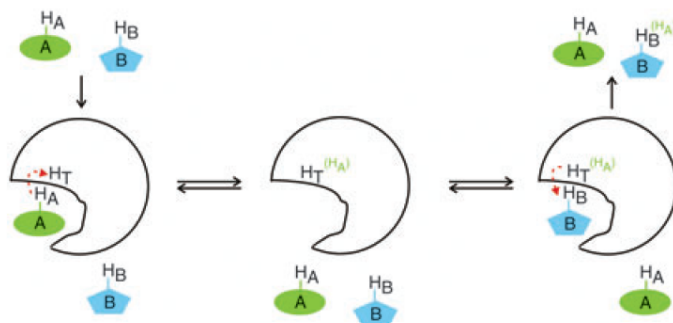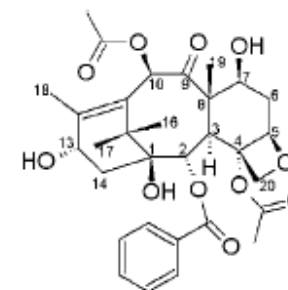epothilone A (E)   baccatin III (B)

Tubulins are targets for anticancer drugs like Taxol and the "Vinca alkaloid" drugs such as vinblastine and vincristine. The anti-gout agent colchicine binds to tubulin and inhibits microtubule formation, arresting neutrophil motility and decreasing inflammation. The anti-fungal drug Griseofulvin targets mictotubule formation and has applications in cancer treatment.

41
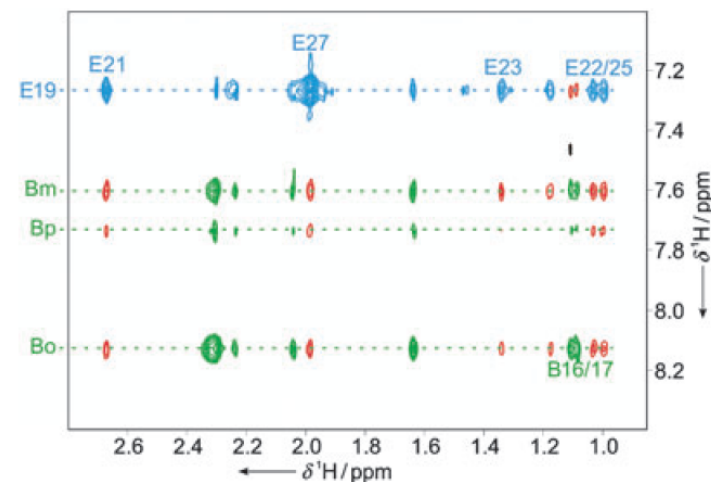
Quo vadis?
Kinetic processes - Folding of α-lactalbumin
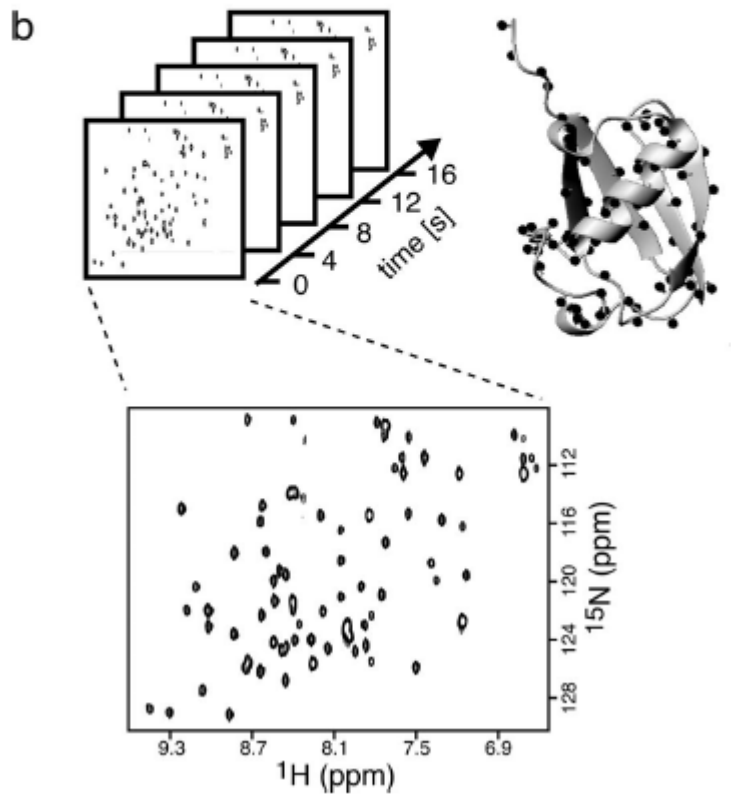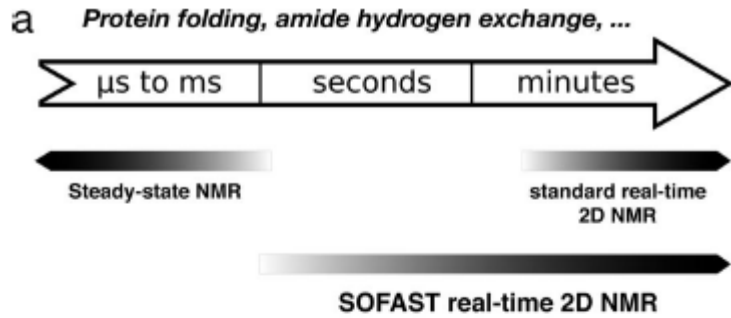
Schanda et al. PNAS 104, 11257- 11262, 2007
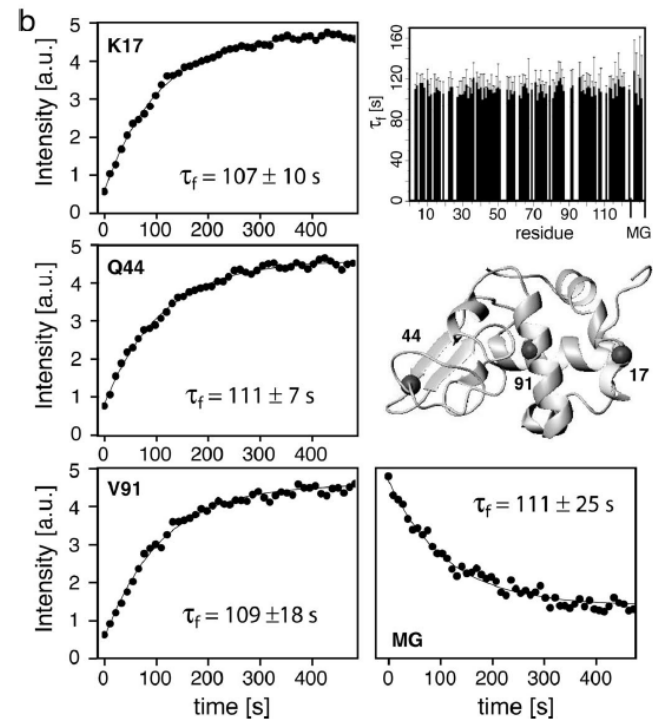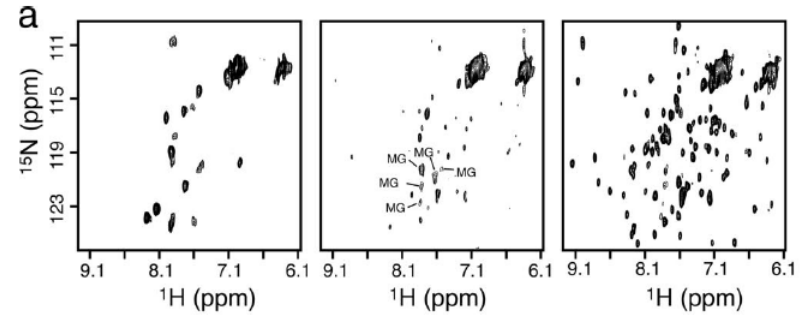
Quo vadis?
Structure and dynamics of a ribosome-bound nascent chain by NMR spectroscopy
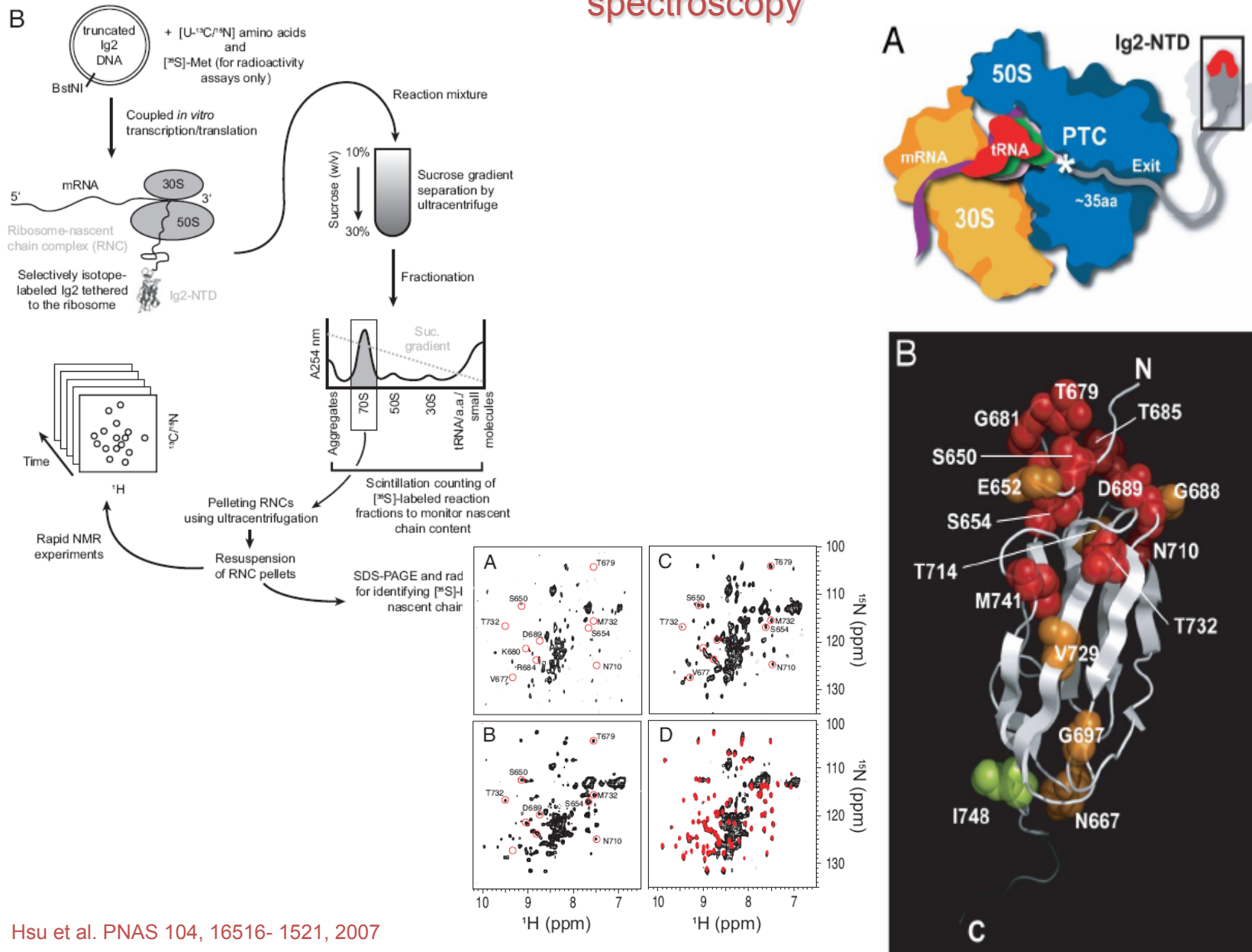
Quo vadis?
Structure and function of biomacromolecules in living cells or cell extracts
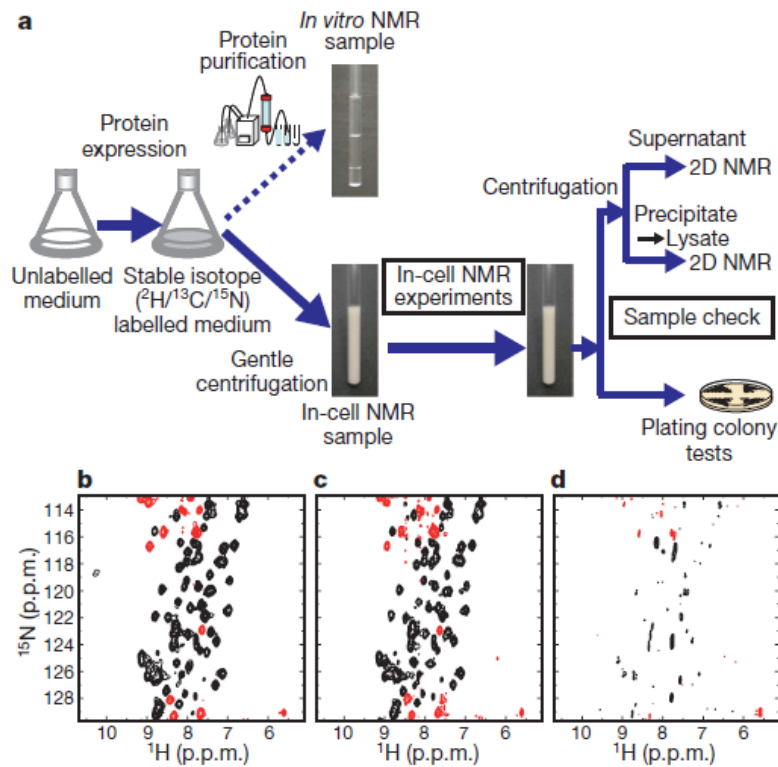
Yutaka Ito et al. Nature 458, 102-106, 2009
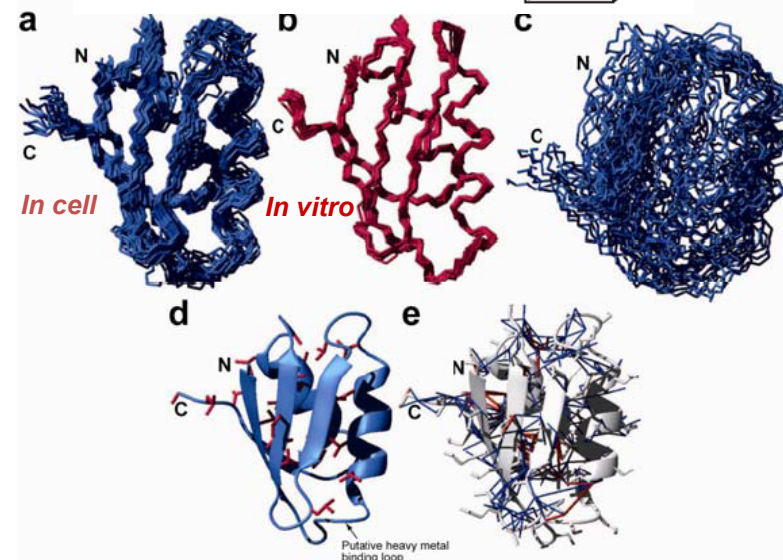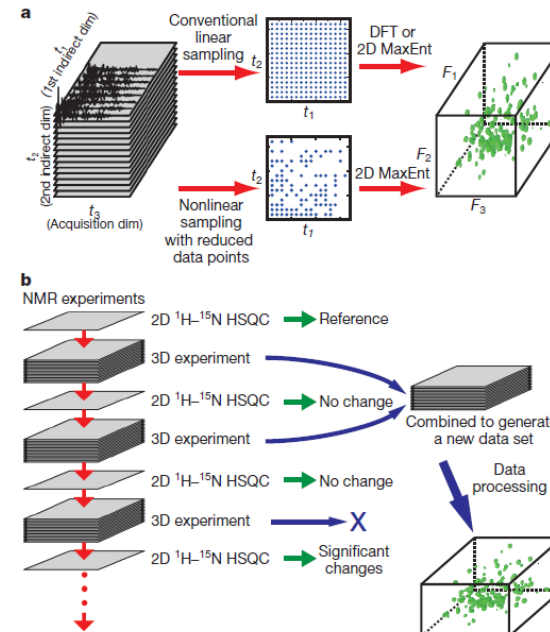
NMR solution structure of TTHA1718 in living *E. coli* cells.
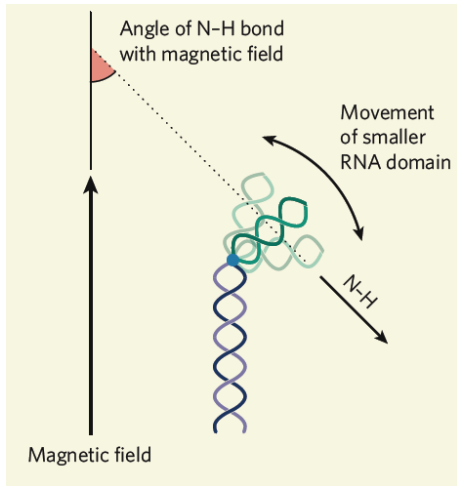
Quo Vadis
Dynamics from Residual Dipolar Couplings
Molecular motions on μs time scale

HIV TAR
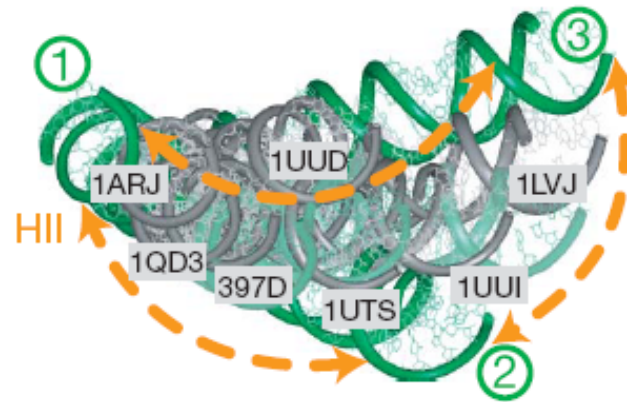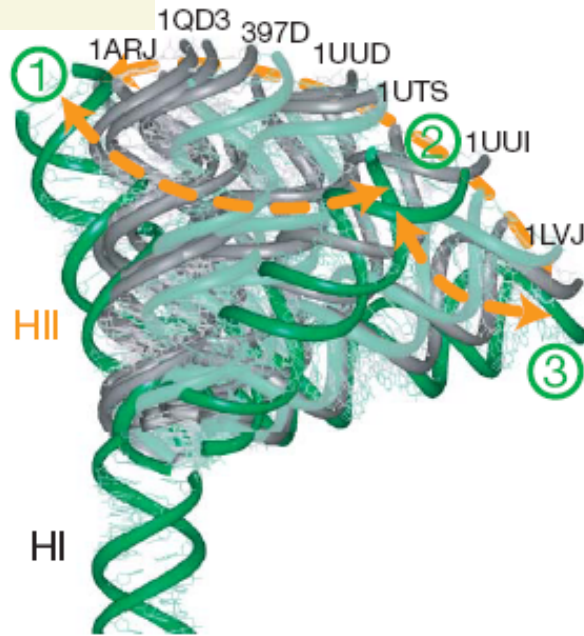
Comparison of the three TAR dynamical conformers (green) and ligand-bound TAR conformations (grey). Sub-conformers along the linear pathway linking conformers 1R2, 2R3 and 3R1 are shown in light green, and the direction of the trajectory is shown with arrows.

Qui Zhang et al. Nature, 450, 1263 (2007)

Quo Vadis
Dynamics from Residual Dipolar Couplings
Molecular motions on μs time scale
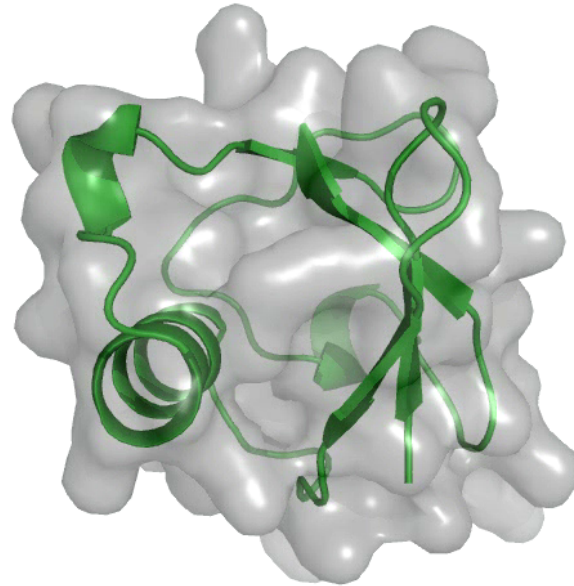
46 ubiquitin structures

Induced Fit
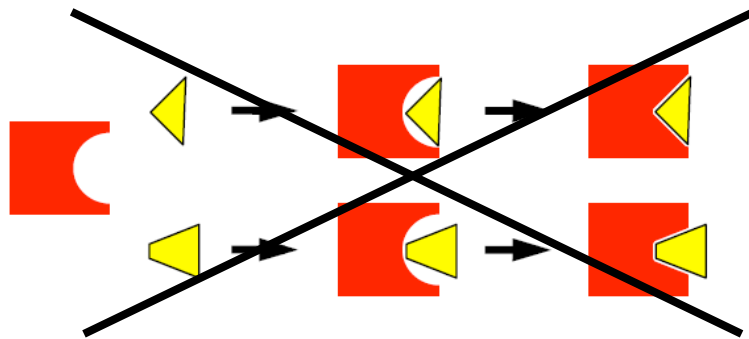
Conformational Selection
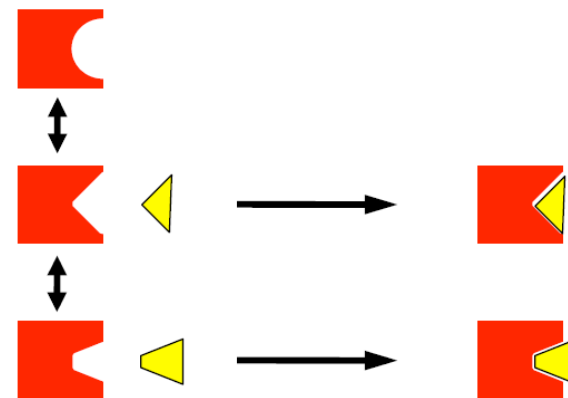
Recognition mechanisms

46

Quo vadis?
3D protein structures by solid-state NMR

magnetic field 54.7°
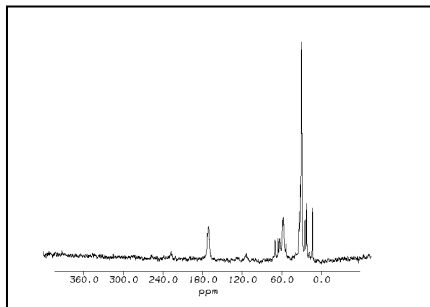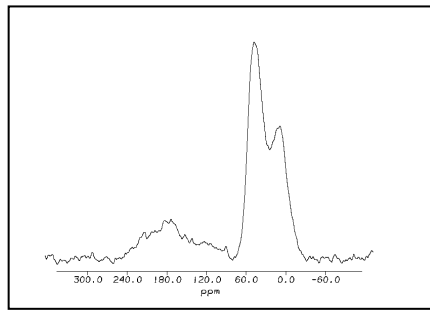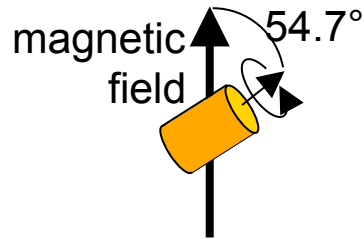
MAS: ^{13}C –NMR of ^{13}C, ^{15}N labelled peptide in hydrated DMPC bilayer with and without sample spinning

Wasmer, C., Lange, A., Van Melckebeke, H., Siemer, A.B., Riek. R., Meier. B.H. Amyloid fibrils of the HET-s(218-289) prion form a beta solenoid with a triangular hydrophobic core
Science **319,** 1523-1526, 2008
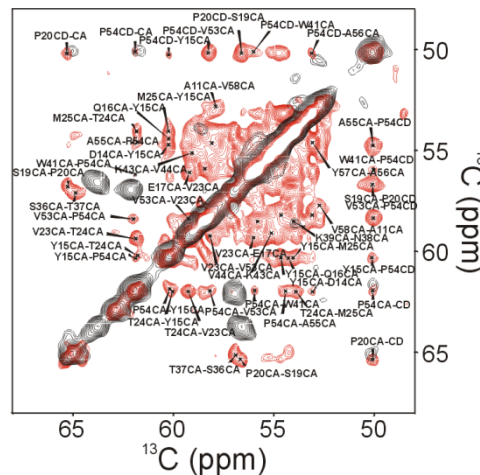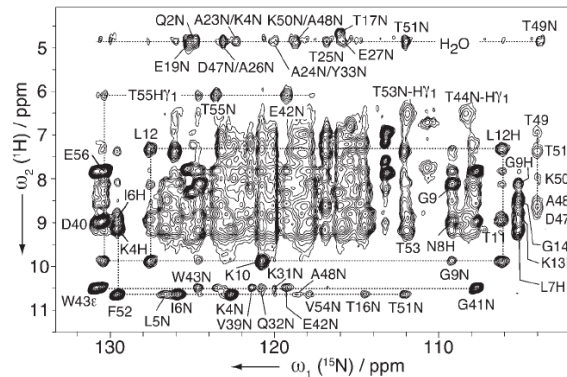
[U-^{13}C]glycerol SH3

[2-^{13}C]glycerol SH3

NMR

X-ray
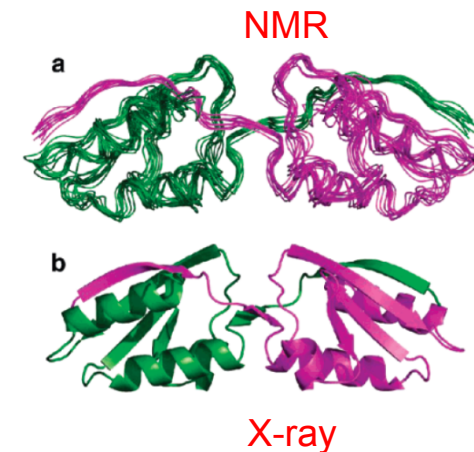
Loquet. A., Bardiaux. B., Gardiennet. C., Blanchet. C., Baldus. M., Nilges. M., Malliavin. T., Bockmann. A.
3D structure determination of the Crh protein from highly ambiguous solid-state NMR restraints. J.Am.Chem.Soc. **130,** 3579-3589, 2008.

47

Quo vadis?
Biomolecular NMR methodology

TROSY

CRINEPT
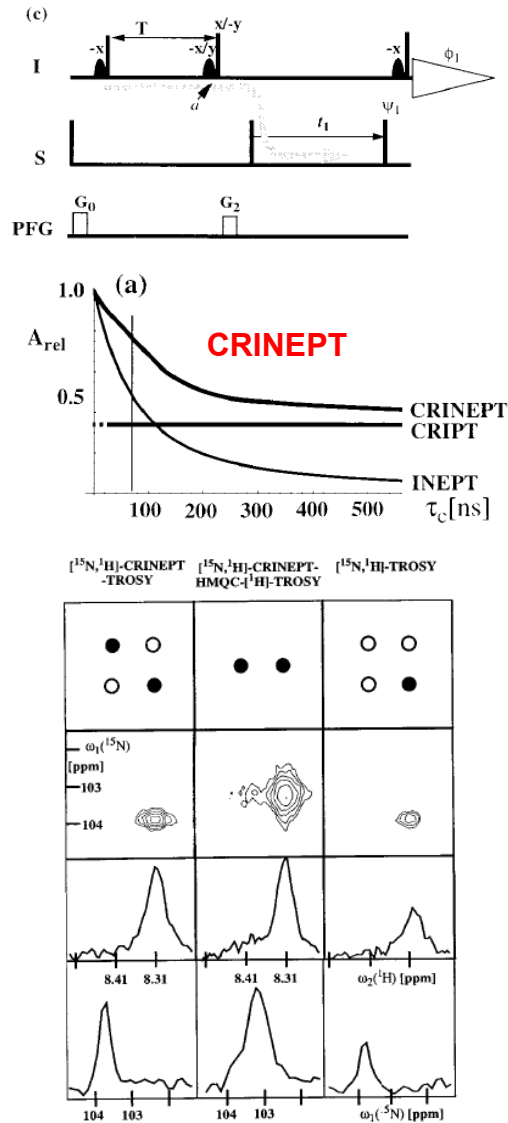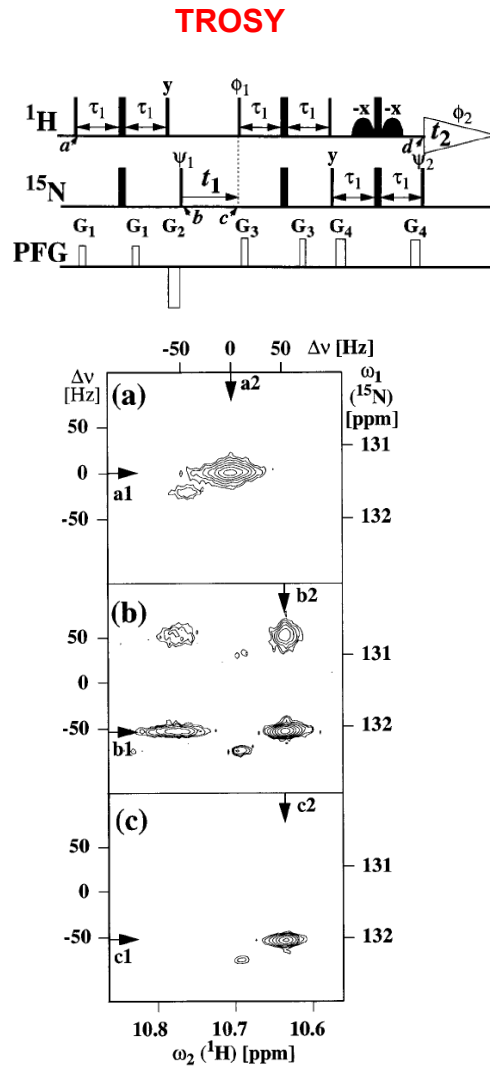
[u-15N, 75% ^{2}H]-labeled *S. aureus* aldolase a 110 kDa protein, τ_c > 70 ns

SAIL isotope labeling
stereo-array isotope labeling
cell-free expression

Pervushin et al. PNAS 92, 12366-12371, 1997   Riek et al. PNAS 96, 4918-4923, 1999   Kainosho et al. Nature 440, 52-57, 2006
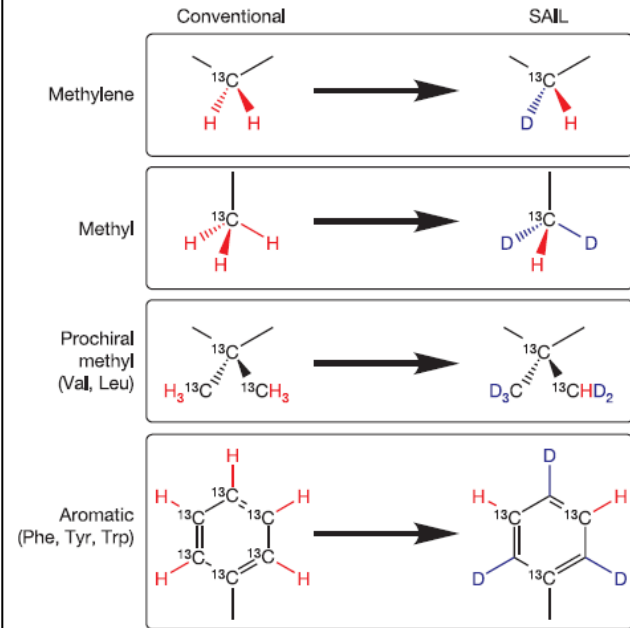
Quo vadis?
Biomolecular NMR methodology

Reduced dimensionality, GFT NMR

- GFT NMR = reduced dimensionality with quadrature detection

3D FT NMR

(3,2) GFT NMR
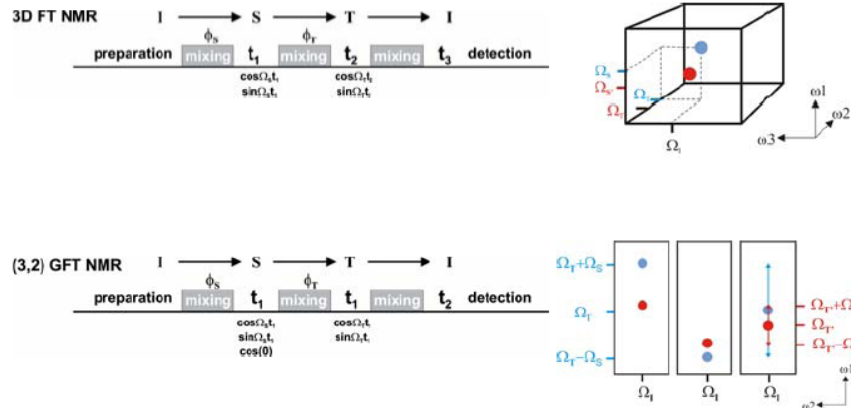
Projection reconstruction

- Record lower dimensionality projections of ND spectra ➔ time saving
  - 1) Reconstruction of ND object (spectrum) from projections (as in tomography)
    i.e. using lower value algorithm (Kupce & Freeman)
  - 2) ND peak list from projections without reconstruction (APSY, Wider et al.)

Projection reconstruction theorem

A skewed projection with angle α of a 2D frequency domain corresponds to the FT of a skew cross-section through the origin of the 2D time domain with angle α.
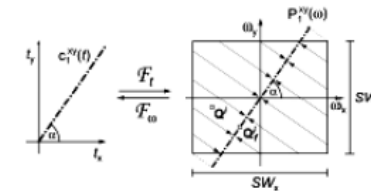
2D projection of the two indirect dimensions of a 3D experiment with angle α involves simultaneous evolution of the indirect time dimensions t_1, t_2 with increments: $\Delta t_2 \cos(\alpha)$ and $\Delta t_1 \sin(\alpha)$

Single-scan nD acquisition
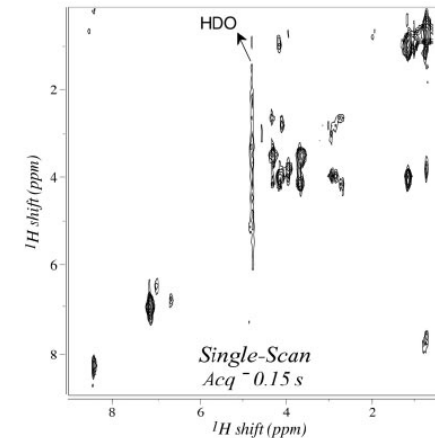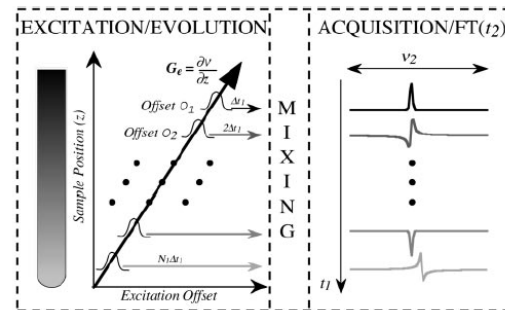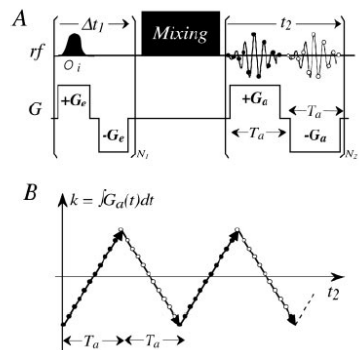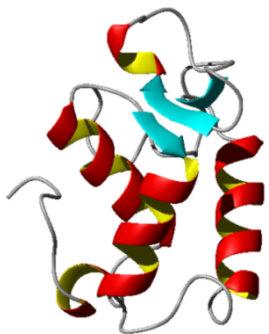
Quo vadis?
Non-linear sampling

δsubunit of RNA polymerase
with an **unstructured** C-tail (57 aa)
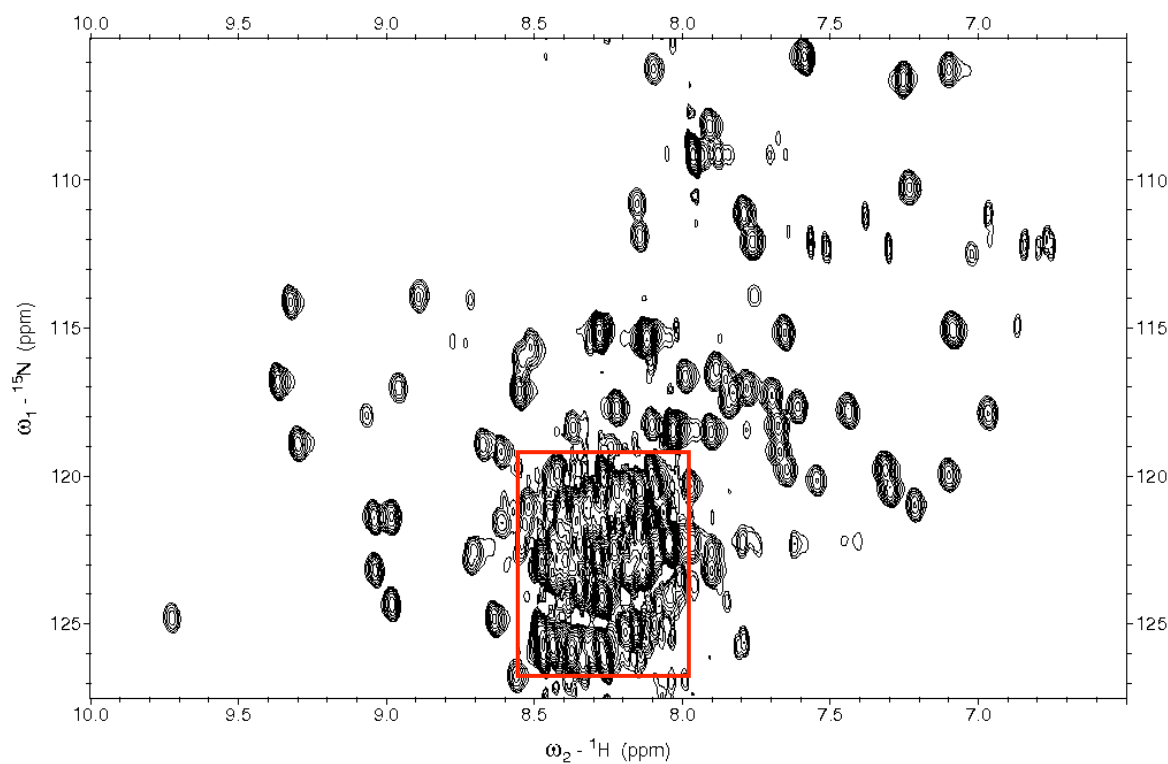
2D projection of 3D HNCO
Linear sampling 20 hours
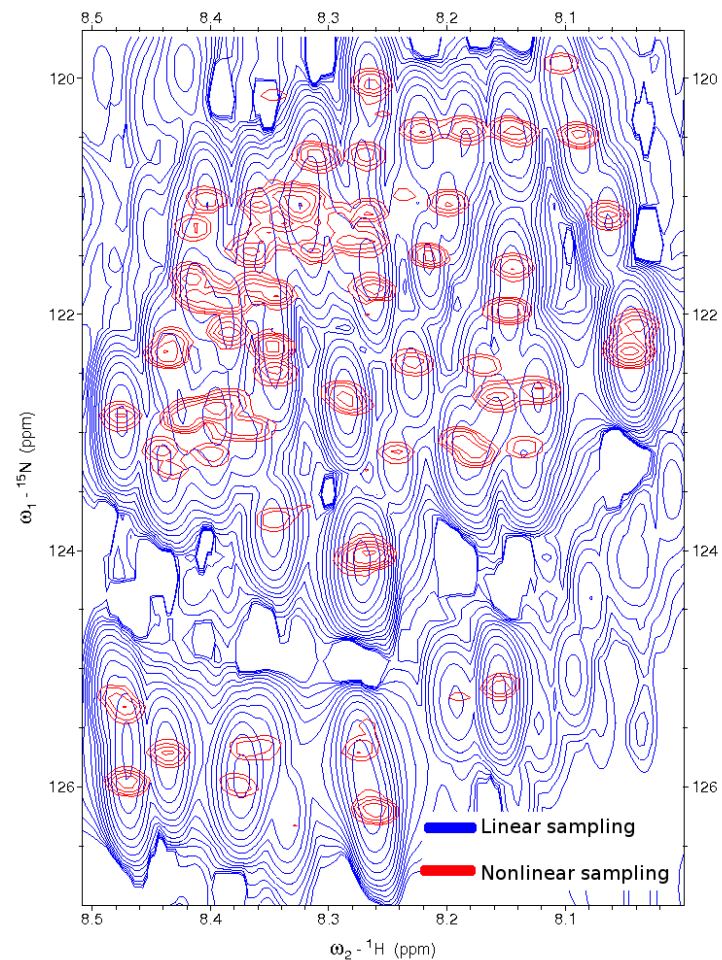
2D projection of 3D HNCO
Non-linear sampling 3 hours

Quo vadis?
Biomolecular NMR methodology

DNP – Dynamic Nuclear Polarization

800 ms laser pulse

In Situ Temperature-Jump DNP
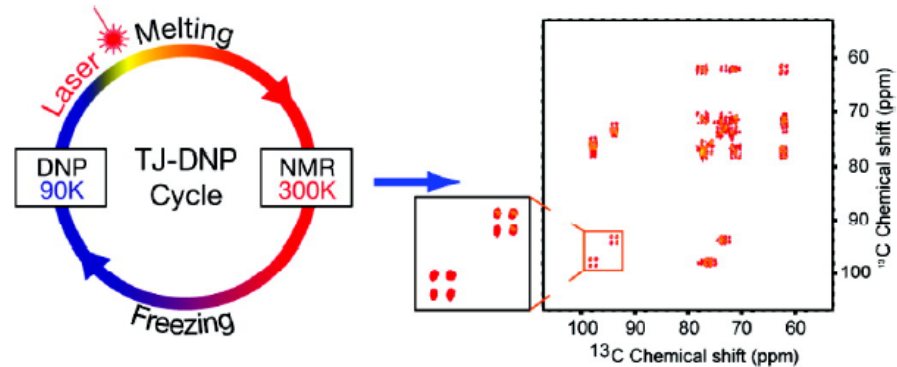
40 s freezing by N$_2$ gas
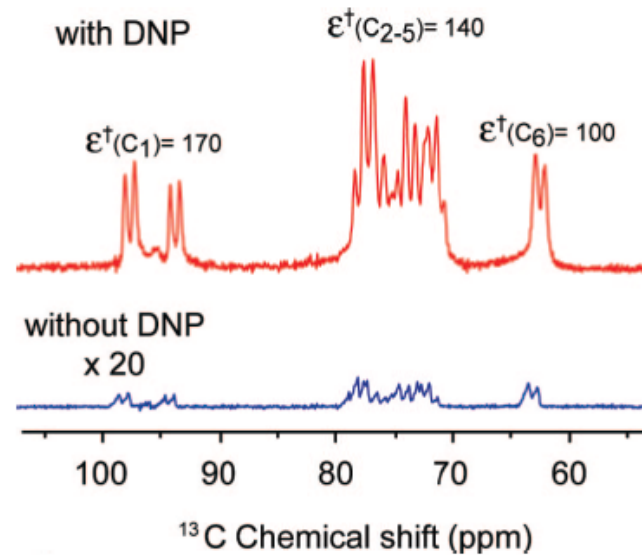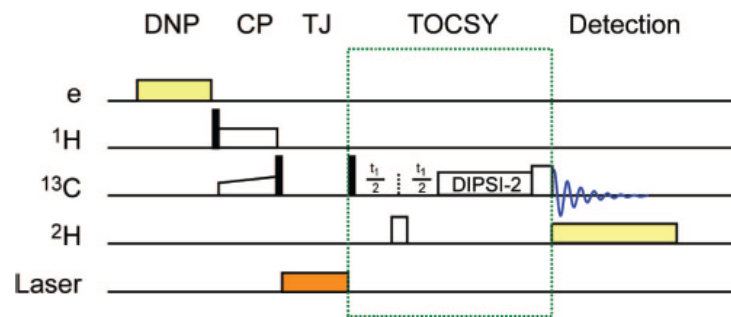
Quo vadis NMR?

Current challenges

• study of molecular complexes of increasing size and complexity

• characterization of weakly interacting molecular networks

• investigation of structural preferences in natively unstructured proteins

• observation of kinetic processes and excited state conformations involved in protein folding, binding, and allosteric signal transduction

• studies of structure and function in living cells or cell extracts

• studies of molecular motions on μs -ms time scale in complex assemblies

• structure determination in solid state polycrystalline samples

• structure determination of membrane proteins using solid state technology

Quo vadis NMR?

Forward, future is bright

Magic Spin Gymnastics

3D HsCNbCHb experiment MQ-TROSY
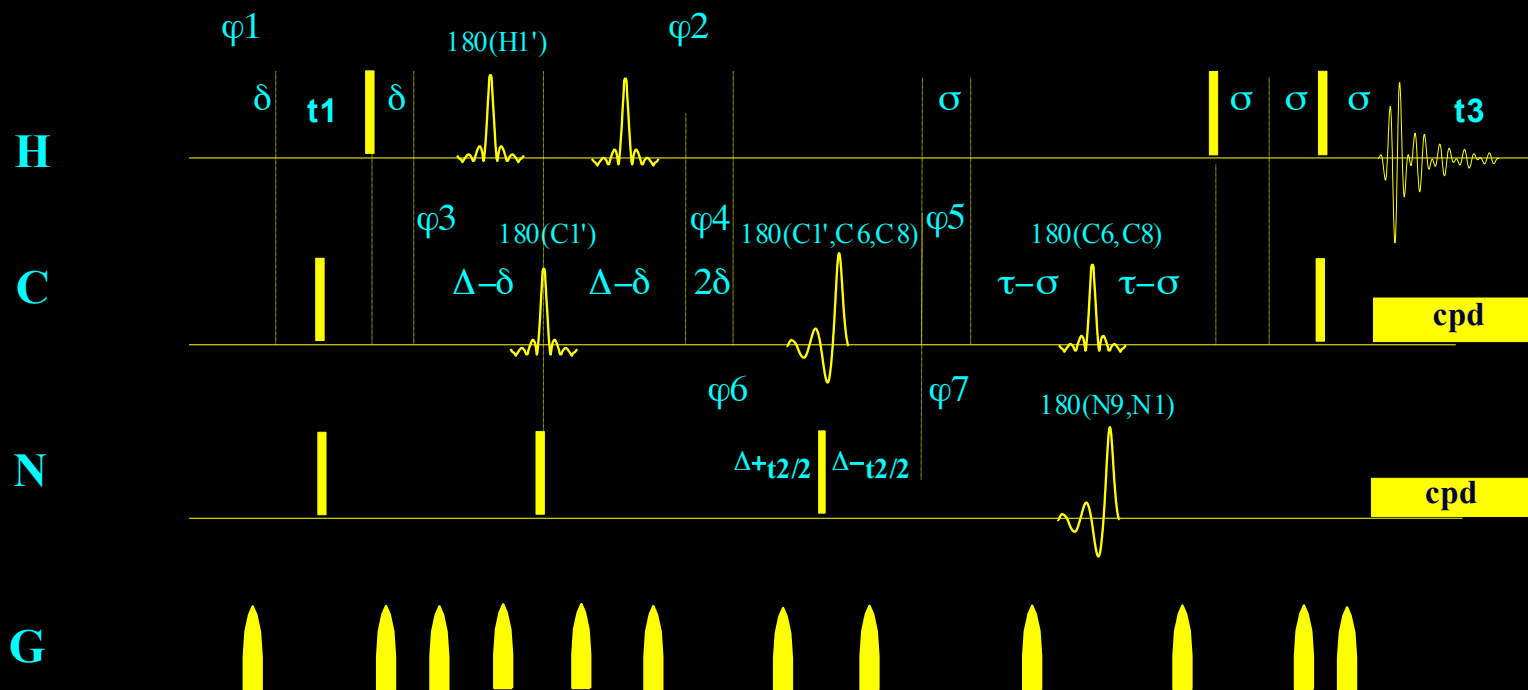
NMR Laboratory

Bruker *Avance*

1995

1999

2001

500 MHz

300 MHz

600 MHz

Structural Biology

prof. Vladimír Sklenář

Programme coordinator

EUROPEAN UNION
EUROPEAN REGIONAL DEVELOPMENT FUND
INVESTING IN YOUR FUTURE

OP Research and
Development for Innovation

Vision

Structural Biology Program will integrate information on the structure of biologically important macromolecules - proteins, nucleic acids and their complexes. The aim is to obtain the knowledge necessary to understand the basic functions and life processes at the molecular and cellular levels. Progressive high-resolution methods of structural analysis such as X-ray diffraction, nuclear magnetic resonance, cryo-electron microscopy and tomography will be used in combination with modern methods of molecular modelling, theoretical chemistry, and bioinformatics. Time variations of three-dimensional structures, supplying essential information indispensable for painting a dynamic picture of key cellular functions, will be investigated in detail.

X-ray
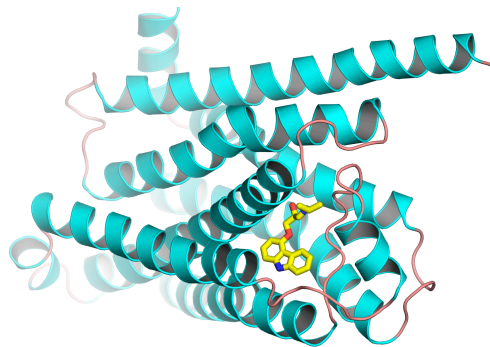
NMR
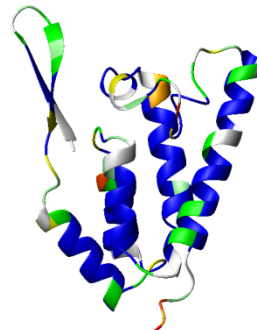
Cryo-EM & tomography

57
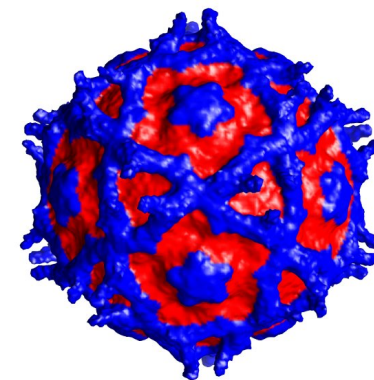
Vision

A new integrated infrastructure built within CEITEC will be used to develop modern methods of structural biology and to extract molecular data crucial for biochemical and biomedical applications. The Structural Biology programme is aimed at achieving European competitiveness, stimulate regional development and facilitate biomedical research and biotechnologies. At the application level, its results will facilitate developments of the next-generation diagnostic and therapeutic strategies for the treatment of human diseases and solutions of health problems.

integrative approaches
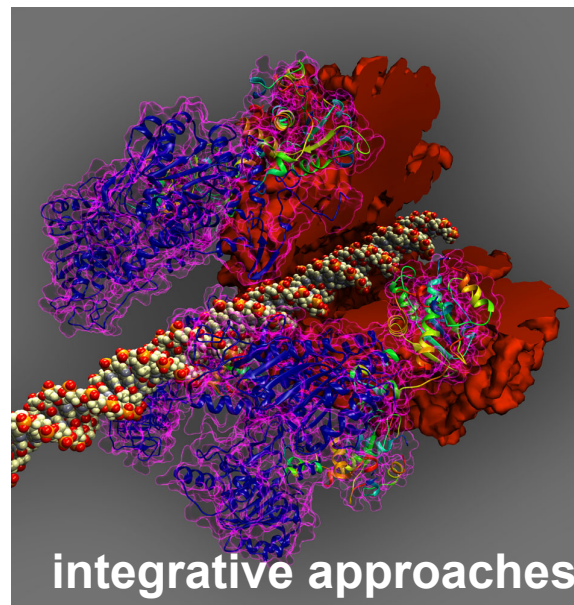
Vision

INSTRUCT - Integrated Structural Biology Infrastructure for Europe
ESFRI project

instruct
Integrating
Biology

Czech Infrastructure for Integrative Structural Biology

Goal: National Affiliate Centre (approved 2011) → INSTRUCT Centre (2015)

CEITEC
central european institute of technology
BRNO | CZECH REPUBLIC

BioCeV

NMR
X-ray crystallography
Cryo-electron microscopy and tomography
Biophysical investigations

X-ray crystallography
Mass spectrometry
Structural Bioinformatics

5   2007–13
OP Výzkum a vývoj
pro inovace

Vision

CEITEC

ELIXIR - Infrastructure for biological information in Europe
ESFRI project

Czech ELIXIR node

Czech Republic National Roadmap for Research Infrastructures

Bioinformatics
Computational Chemistry

ÚOCHB AV ČR, v.v.i.

CESNET

CERIT

VŠCHT PRAHA

Research objectives

CEITEC

- Investigation of the role of RNA in development and human diseases.

- To study the therapeutical aspects of recognition and adhesion phenomena in host-pathogen interactions.

- The visualization and modification of biological objects including tissues, cells, cellular structures, and biomolecules.

- The development of new methodologies for investigating the structure, interactions, and dynamics of biomolecules.

- High throughput structural characterization of macromolecular assemblies by single-crystal diffraction.

Research objectives

- **To establish a bioinformatics laboratory focussing on gene expression profiling and sequence analysis.**

- **To establish a high-end cryo electron microscopy laboratory for highly sophisticated 3D imaging studies for structural biology at the cellular level.**

- **Investigations of the structure and interactions of biomacromolecules and their relation to the functions of living systems, disease and therapy.**

- **Investigations of the behaviour of natural and chemically modified biomacromolecules at electrically charged surfaces linked to the development of novel electrochemical biosensors and bioassays.**

- **The enhancement of the theoretical background to the design, synthesis and clinical use of novel anticancer and antiviral therapeutics.**

Work Packages

CEITEC

WP-3-1 | Structural and molecular biology of RNA

WP-3-2 | Structural and molecular biology of host-pathogen interactions

WP-3-3 | Nanobiotechnology for Health

WP-3-4 | New methods for structural biology

WP-3-5 | Protein crystallography

WP-3-6 | Gene expression profiling and sequence analysis

WP-3-7 | Cryo electron microscopy and tomography of cellular biopolymers

WP-3-8 | Biophysics and biophysical chemistry of biopolymers and their interactions

Research Groups | Research Group Leaders

CEITEC

- **RG-3-01 |** Bioinformatics | **Hedi Hegyi**
- RG-3-02 | CD Spectroscopy of Nucleic Acids and Proteins | **Michaela Vorlíčková**
- **RG-3-03 |** Cryo-EM | **Jürgen Plitzko**
- RG-3-04 | Glycobiochemistry | **Michaela Wimmerová**
- RG-3-05 | RNA Quality Control | **Štěpánka Vaňáčová**
- RG-3-06 | Nanobiotechnology | **Petr Skládal**
- RG-3-07 | Biomolecular NMR Spectroscopy | **Vladimír Sklenář**
- **RG-3-08 |** RNA-based regulation of gene expression | **Peter J. Lukavsky**
- RG-3-10 | Structural biology of gene regulation | **Richard Štefl**
- **RG-3-12 |** Structural Virology | **Pavel Plevka**
- RG-3-13 | Structure and Dynamics of Nucleic Acids | **Jiří Šponer**
- RG-3-14 | Structure and Interaction of Biomolecules at Surfaces | **Miroslav Fojta**
- RG-3-15 | Computational Chemistry | **Jaroslav Koča**

Core Facilities
Josef Dadok National NMR Centre

- **950 MHz NMR with a cryoprobe for high-resolution spectroscopy in liquids**

- **850 MHz NMR with a cryoprobe for high-resolution spectroscopy in liquids**

- **700 MHz NMR with a cryoprobe for high-resolution spectroscopy in liquids**

- **700 MHz NMR for high resolution NMR in liquids and solids**

- **Upgrade of existing 600 MHz NMR with a cryoprobe for high-resolution spectroscopy in liquids**

- **Upgrade of existing 500 MHz NMR with a cryoprobe for high-resolution spectroscopy in liquids and solids**

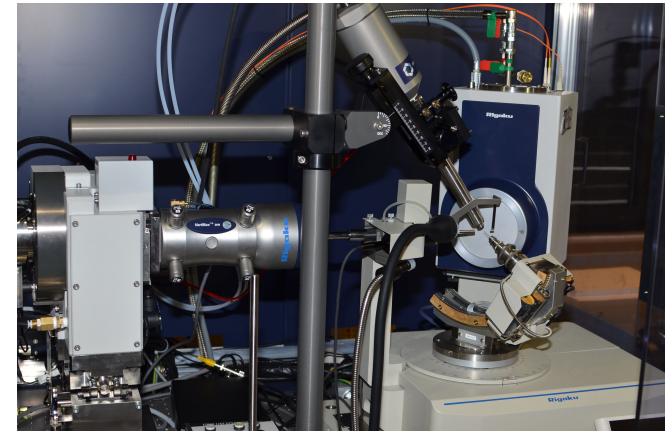- **Operational since November 2012**

Core Facilities
X-ray/Bio-SAXS

- **2 RIGAKU diffractometers with rotating anode**

- **One robotized protein diffractometer**
- **Universal mono-crystal diffractometer**

- **Crystal preparation**

- **Robotized crystallization laboratory**
- **Crystallization laboratory equipment**
- **X-ray and optical protein scanner**

Core Facilities
Biomolecular Interactions

- **Equipment planned for Biomolecular interactions CF**

    – **microcalorimeter AutoITC$_{200}$ (GE Healthcare)**
       – in full operation since March 2013

    – **Semi-automated SPR system (GE Healthcare SPR Biacore T100, T200?) - tender in preparation**

    – **SPR biosensors for multiplex measurements (Horiba Openplex, BioRad ProteOn XPR36?
       - tender in preparation**

- **In the meantime, instrumentation purchased from other resources is offered:**

    – **microcalorimeters VP-ITC, VP-DSC, ITC200 (GE Healthcare)**

    – **SPR biosensor Biacore 3000 (GE Healthcare)**

    – **Analytical ultracentrifuge ProteomLam XLI (Beckman-Coulter)**

    – **CD spectrophotometer J-815 (Jasco) equipped with fluorescence and stopped-flow (Biologic)**
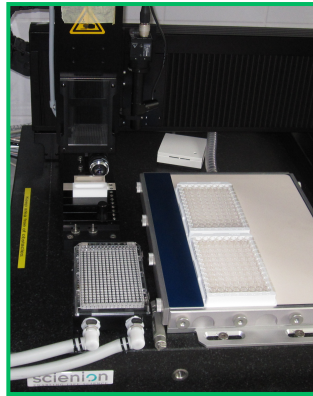

AutoITC$_{200}$

Core Facilities
Nanobio

CEITEC

Currently available instrumentation:

- **Atomic force microscope**
  - **Nanowizard3 + ForceRobot300 (JPK)**
  - **to be mounted on the confocal fluorescence microscope IX81/FV1000 (Olympus)**
- **Deposition and immobilization of biomolecules**
  - **sciFLEXARRAYERS S1 and S3 (Scienion)**

Tenders:

- **in progress: fully automated AFM (edu level), electrochemical / nanolithographic modules for current AFM Ntegra Vita**
- **in preparation: electrochemical analyzer (entry level, repeated)**
- **high-resolution fluorescence scanner**
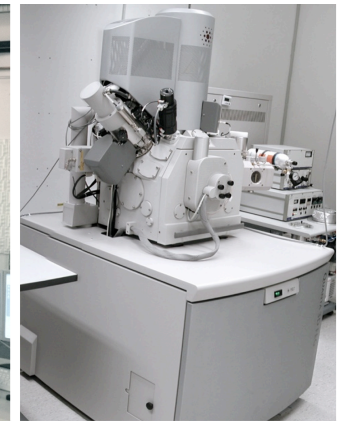
Core Facilities
cryo-EM

- **Titan Krios (the voltage range of 80 to 300kV) for high throughput single particle acquisition as well as for cellular tomography purposes**

- **Tecnai F20 for computer assisted single particle acquisition or tomography of thinner objects (small prokaryotic cells or sections) as well as for tomography of macromolecular complexes to determine their higher-order structure.**

- **FIB Versa 3D for micromachining and milling thin lamellas of cryo specimens, such as intracellular compartments, suitable for cryo-electron tomography**

- **Vitrobot Mark IV for reproducible and environmentally controlled sample preparation of frozen hydrated EM grids of cells or purified and isolated macromolecular complexes**

TITAN KRIOS · Tecnai F20 · FIB Versa 3D

Vitrobot Mark IV 69